

Approximating Quasiparticle and Excitation Energies from Ground State Generalized Kohn-Sham Calculations

Yuncai Mei,[†] Chen Li,[†] Neil Qiang Su,[†] and Weitao Yang^{*,†,‡}

[†]*Department of Chemistry, Duke University, Durham, NC 27708*

[‡]*Key Laboratory of Theoretical Chemistry of Environment, School of Chemistry and
Environment, South China Normal University, Guangzhou 510006, China*

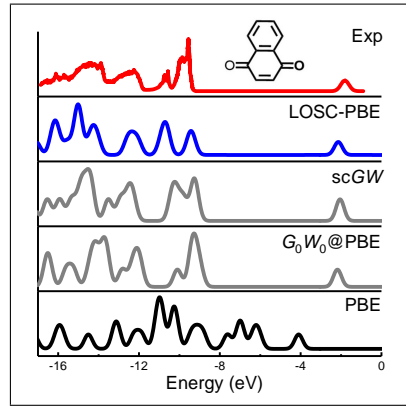
E-mail: weitao.yang@duke.edu

March 17, 2022

Abstract

Quasiparticle energies and fundamental band gaps in particular are critical properties of molecules and materials. It was rigorously established that the generalized Kohn-Sham HOMO and LUMO orbital energies are the chemical potentials of electron removal and addition and thus good approximations to band edges and fundamental gaps from a density functional approximation (DFA) with minimal delocalization error. For other quasiparticle energies, their connection to the generalized Kohn-Sham orbital energies has not been established but remains highly interesting. We provide the comparison of experimental quasiparticle energies for many finite systems with calculations from the GW Green's function and localized orbitals scaling correction (LOSC), a recently developed correction to semilocal DFAs, which has minimal delocalization error. Extensive results with over forty systems clearly show that LOSC orbital energies achieve slightly better accuracy than the GW calculations with little dependence on the semilocal DFA, supporting the use of LOSC DFA orbital energies to predict quasiparticle energies. This also leads to the calculations of excitation energies of the N -electron systems from the ground state DFA calculations of the $(N - 1)$ -electron systems. Results show good performance with accuracy similar to TDDFT and the delta SCF approach for valence excitations with commonly used DFAs with or without LOSC. For Rydberg states, good accuracy was obtained only with the use of LOSC DFA. This work highlights the pathway to quasiparticle and excitation energies from ground density functional calculations.

Graphical TOC Entry



Quasiparticles are a powerful concept in electronic structure theory of many-electron systems. In particular, accurate prediction of quasiparticle energies is essential for interpreting the electronic excitation spectra of molecules and materials, such as photoemission and optical experiments. Formally, quasiparticle energies can be exactly formulated in many-body perturbation theory.^{1–3} In practice, the GW approximation^{4–7} is most widely used for bulk simulations. Unfortunately, GW calculations are still expensive computationally. Therefore, a low-cost alternative to GW approximation that offers good accuracy for the prediction of quasiparticle energies is critical to the calculations of large-scale systems, and for efficient high throughput study of materials.

Kohn-Sham (KS) density functional theory (DFT),^{8–10} due to its good balance between accuracy and computational tractability, is among the most popular and versatile methods available for many-electron problems. In addition to the total electron energy, the physical interpretation of the KS eigenvalues has also attracted great interest. It has been known for decades that among the KS eigenvalues obtained from the exact functional, the highest occupied molecular orbital (HOMO) energy, $\varepsilon_{\text{HOMO}}$, is negative vertical ionization potential (VIP), $-I$.^{10–17} In 2008, it was rigorously proven^{18,19} that within the generalized KS (GKS) theory, which includes KS theory as a special case, the HOMO/LUMO energy is the chemical potential, $(\frac{\partial E}{\partial N})_v$, for electron removal/addition from the DFAs for any DFA that is a differentiable functional of the non-interacting one-electron density matrix in case of GKS or the density in case of KS, and consequently approximation to $-I/A$ following the Perdew-Parr-Levy-Balduz (PPLB) condition.^{11,20–22} Accurate approximation of $-I/A$ can thus be expected from the HOMO/LUMO energy of DFAs with minimum delocalization error.²³ Therefore, the fundamental gap defined as $I - A$ can be exactly obtained from the chemical potential difference, that is, the GKS HOMO-LUMO gap.

In addition to HOMO and LUMO, the physical meaning of other GKS eigenvalues also has great theoretical significance and application value. Of particular interest is the connection between the GKS spectrum and the quasiparticle spectrum. Unfortunately, no clear

connection has been established, although there have been many attempts to approximately attach some meanings to the occupied orbital energies within the KS theory. It has been argued that the orbital energies below $\varepsilon_{\text{HOMO}}$ can be interpreted as other approximate principle (sometimes called relaxed) VIPs, i.e., the ionized system being in an excited state.^{24,25} Recently, it has been argued that the correct occupied KS orbital energies should correspond to the exact principle VIPs using the linear response time-dependent density functional theory (LR-TDDFT) under the adiabatic approximation.^{26–28} However, it has been shown that the adiabatic approximation within TDDFT is not generally valid.²⁹

Even though no theorem has been rigorously established to link the remaining GKS orbital energies to quasiparticle energies, it is still beneficial for practical applications to construct a good density functional approximation (DFA) that can accurately predict quasiparticle energies from orbital energies. For commonly used DFAs, such as local density approximations (LDAs), generalized gradient approximations (GGAs) and hybrid GGAs, their HOMO and LUMO energies are the corresponding chemical potentials but have large systematic error in predicting $-I / -A$.^{18,23} In particular, the HOMO energy is significantly overestimated, which leads to underestimation of I ; while the LUMO energy is severely underestimated, so that A is overestimated. Hence, the fundamental gap is significantly underestimated by HOMO-LUMO gap of common DFAs. From the fractional charge perspective, this failure has been attributed^{18,23} to the violation of the PPLB condition^{11,20–22} which requires the total energy, as a function of electron number, to be piecewise straight lines interpolating between adjacent integer points. And the convex deviation suffered by commonly used DFAs was identified as the delocalization error inherent in approximate functionals.^{23,30,31} Other occupied and unoccupied orbitals follow the same trend as HOMO and LUMO, respectively. Typically, energies of occupied orbitals (including HOMO) have been seriously overestimated when serving as approximations to electron removal energies, so that they cannot qualitatively reproduce experimental photoemission spectrum. It is thus reasonable to believe that other orbitals should suffer similarly from the delocalization error

of approximate functionals.

Following the perspective of fractional charges, there have been many attempts focusing on removing delocalization error in approximate functionals. MCY3³² was the first DFA constructed to restore the PPLB condition; long-range corrected (LC) functionals^{33–36} and doubly hybrid functionals^{37–39} show some promise on reproducing linear fractional charge behavior; tuned range-separated hybrid functionals^{40,41} impose extra constraints on orbital energies from total energy difference by optimizing the range-separation parameter for each system. All these functionals show significantly improvement on the calculations of HOMO and LUMO energies for small molecules. Extension to large and bulk systems lead to various issues. To achieve systematic elimination of the delocalization error associated with commonly used DFAs, recently developed localized orbital scaling correction (LOSC) functional⁴² introduces a set of auxiliary localized orbitals (LOs), or orbitalets, and imposes PPLB condition on each of the LOs. As a result, LOSC can achieve size-consistent corrections to both the total energy and orbital energies.

To demonstrate that orbital energies $\varepsilon(N)$ of LOSC can give accurate approximation to quasiparticle/quasihole energies $\omega^{+/-}(N)$ for an N -electron system, for the description of electron addition/removal, i.e.

$$\begin{aligned}\varepsilon_m(N) &\approx \omega_m^+(N) = E_m(N+1) - E_0(N), \\ \varepsilon_n(N) &\approx \omega_n^-(N) = E_0(N) - E_n(N-1),\end{aligned}\tag{1}$$

we have already applied LOSC to generate accurate LUMO and HOMO energies for a broad range of atoms and molecules.⁴² In Eq. 1, $\varepsilon_m(N)/\varepsilon_n(N)$ is a virtual/occupied GKS orbital energy for the N -electron system. The performance of LOSC for HOMO/LUMO and other GKS orbital energies will be examined extensively in present work.

Furthermore, Eq. 1 allows the calculation of excitation energies $\Delta E_m(N)$ at the cost of

a ground-state DFT calculation via the particle part of the quasiparticle spectrum of the $(N - 1)$ system, i.e.

$$\begin{aligned}
\Delta E_m(N) &= E_m(N) - E_0(N) \\
&= [E_m(N) - E_0(N - 1)] - [E_0(N) - E_0(N - 1)] \\
&= \omega_m^+(N - 1) - \omega_{min}^+(N - 1) \\
&\approx \varepsilon_m(N - 1) - \varepsilon_{LUMO}(N - 1),
\end{aligned} \tag{2}$$

where $E_m(N)$ corresponds to the m th excitation of the N -electron system, and $E_0(N - 1)$ is the ground-state energy of $(N - 1)$ -electron system. $E_0(N) - E_0(N - 1)$ is $-A$ of the $(N - 1)$ system and can be obtained from $\omega_{min}^+(N - 1)$, the minimum of particle part of the quasiparticle spectrum, and approximated as $\varepsilon_{LUMO}(N - 1)$, the LUMO energy of the DFA calculation for the $(N - 1)$ system. The excitation energy $\Delta E_m(N)$ can thus be obtained as the virtual orbital energy difference $\varepsilon_m(N - 1) - \varepsilon_{LUMO}(N - 1)$ from a ground-state self-consistent field (SCF) calculation on $(N - 1)$ -electron system. Similarly, excitation energies can also be calculated via the hole part of the quasiparticle spectrum of the $(N + 1)$ system, i.e.

$$\begin{aligned}
\Delta E_n(N) &= E_n(N) - E_0(N) \\
&= [E_0(N + 1) - E_0(N)] - [E_0(N + 1) - E_n(N)] \\
&= \omega_{max}^-(N + 1) - \omega_n^-(N + 1) \\
&\approx \varepsilon_{HOMO}(N + 1) - \varepsilon_n(N + 1),
\end{aligned} \tag{3}$$

where $E_0(N + 1) - E_0(N)$ is $-I$ of the $(N + 1)$ system and can be obtained from $\omega_{max}^-(N + 1)$, the maximum of the hole part in the quasiparticle spectrum, and approximated as $\varepsilon_{HOMO}(N + 1)$, the HOMO energy of the DFA calculation for the $(N + 1)$ system. The

excitation energies can thus be obtained as occupied orbital energy differences $\varepsilon_{HOMO}(N + 1) - \varepsilon_n(N + 1)$ from a ground-state SCF calculation on $(N + 1)$ -electron system.

Many theoretical approaches have been developed to calculate excitation energies. High-level methods, including equation-of-motion coupled cluster (EOM-CC),^{43–45} linear-response coupled cluster (LR-CC),^{46–49} multireference configuration interaction (MRCI),^{50,51} complete active space configuration interaction (CASCI),^{52–54} CASPT2^{55,56} and others, can produce accurate results, but significantly limited in system size and complexity. Other computationally efficient methods, such as configuration interaction singles (CIS),^{57,58} time dependent DFT (TDDFT)⁵⁹ and Δ SCF⁶⁰ have been well-known to describe excitation energies with success, meanwhile they have important weakness. Particularly, CIS can overestimate excitation energy by 2 eV.⁵⁸ TDDFT^{58,61} and Δ SCF method^{62–69} typically yield results with good accuracy, but TDDFT faces challenges to describe double,^{62,70,71} Rydberg^{72–75} and charge transfer excitations.^{76–78} In contrast, Eqs. 2 and 3 provide the simplest way to calculate excitation energies, with which various excitation energies can be obtained after the corresponding ground-state SCF calculation. Obviously, the accuracy of excitation energies from Eqs. 2 and 3 depends on the quality of DFA orbital energies, as approximation to the quasiparticle energies.

Next, we will show the test results of approximating quasiparticle energies (Eq. 1) and excitation energies (Eqs. 2/3) by different DFAs and LOSC-DFAs. For the test of quasiparticle energies, 40 molecules were selected from Blase's⁷⁹ and Marom's⁸⁰ test set to calculate photoemission spectrum, HOMO and LUMO energies. Polyacene ($n=1\text{--}6$) and other three small molecules are used to study the valence orbital energies as approximation to the corresponding quasiparticle energies. For the test of excitation energies, 16 molecules are obtained from Ref. ? as a molecular set to test the low-lying excitation energies. Four atoms (Li, Be, Mg, and Na) are selected as an atomic set to test their excitation energies up to Rydberg states. The QM4D package⁸¹ was used to perform the DFT calculations. Several conventional functionals, such as local density approximation (LDA),^{82,83} PBE,⁸⁴ BLYP^{85,86} and

B3LYP,^{85–87} and LOSC-DFAs were tested. For LOSC calculations, the post-SCF procedure was applied. More details of computations and test results can be found in SI.

Table 1: Mean absolute errors (MAEs, in eV) of orbital energies compared with experimental quasi-particle energies. Experimental reference were obtained from Ref. 79,80.

	HOMO ^a	LUMO ^a	Valence ^b
scGW ^c	0.47	0.34	-
G_0W_0 @PBE ^c	0.51	0.37	-
LOSC_LDA	0.34	0.48	0.69 (0.53)
LOSC_PBE	0.37	0.33	0.60 (0.35)
LOSC_B3LYP	0.26	0.29	0.43 (0.36)
LDA	2.58	2.43	3.06 (2.33)
PBE	2.81	2.16	3.23 (2.55)
B3LYP	2.00	1.57	2.24 (1.79)
Δ -DFA ^d	0.43	0.26	0.70 (0.73)
Δ -LOSC-DFA ^d	0.34	0.38	0.41 (0.26)

^a MAE of HOMO and LUMO energies are based on the results of 40 test molecules.

^b MAE of valence orbital energies (HOMO and below HOMO) are based on 51 states of polyacene ($n = 1 - 6$) and other three small molecules. MAE of polyacene set were listed in the parenthesis.

^c GW results were taken from Ref 80.

^d PBE functional was used in HOMO and LUMO calculation. BLYP functional was used in valence orbital results.

First, HOMO and LUMO energies of different DFAs and LOSC-DFAs are compared. Tab. 1 summarizes mean absolute errors (MAEs) of orbital energies in comparison with experimental quasiparticle energies, where self-consistent GW (scGW)^{5,7} and G0W0^{4,5} results are also included for comparison. Previously, it has been shown that LOSC can size-consistently improve HOMO and LUMO energies on systems range from small sized molecules to polymers.⁴² Here, we further calculated a set of 40 organic molecules, where the molecular size is much larger than that of the G2-97 set tested before. Due to the serious delocalization error,^{18,23} LDA and PBE show systematic underestimation of VIPs and overestimation of VEAs, with MAEs larger than 2.0 eV; hybrid functional B3LYP performs slightly better with a 20% reduction in error, but the results still qualitatively deviate from the experiment. LOSC-DFAs significantly improve both HOMO and LUMO energies, with

MAEs much smaller than their parent DFAs. In particular, MAEs of LOSC-B3LYP are smaller than 0.3 eV. It is also interesting to compare LOSC with the well-recognized scGW and G0W0 methods. We find that LOSC can achieve better accuracy than scGW and G0W0 methods for HOMO and LUMO energy calculations. Our results also show that starting from the same reference DFA (PBE), LOSC (MAE of HOMO 0.37 eV and of LUMO 0.33 eV) outperforms the G0W0 (MAE of HOMO 0.51 eV and of LUMO 0.37 eV). It is well-known that the G0W0 calculation is significantly influenced by the reference DFAs. In contrast, LOSC can provide similar accuracy based on different parent DFAs, including hybrid functionals.

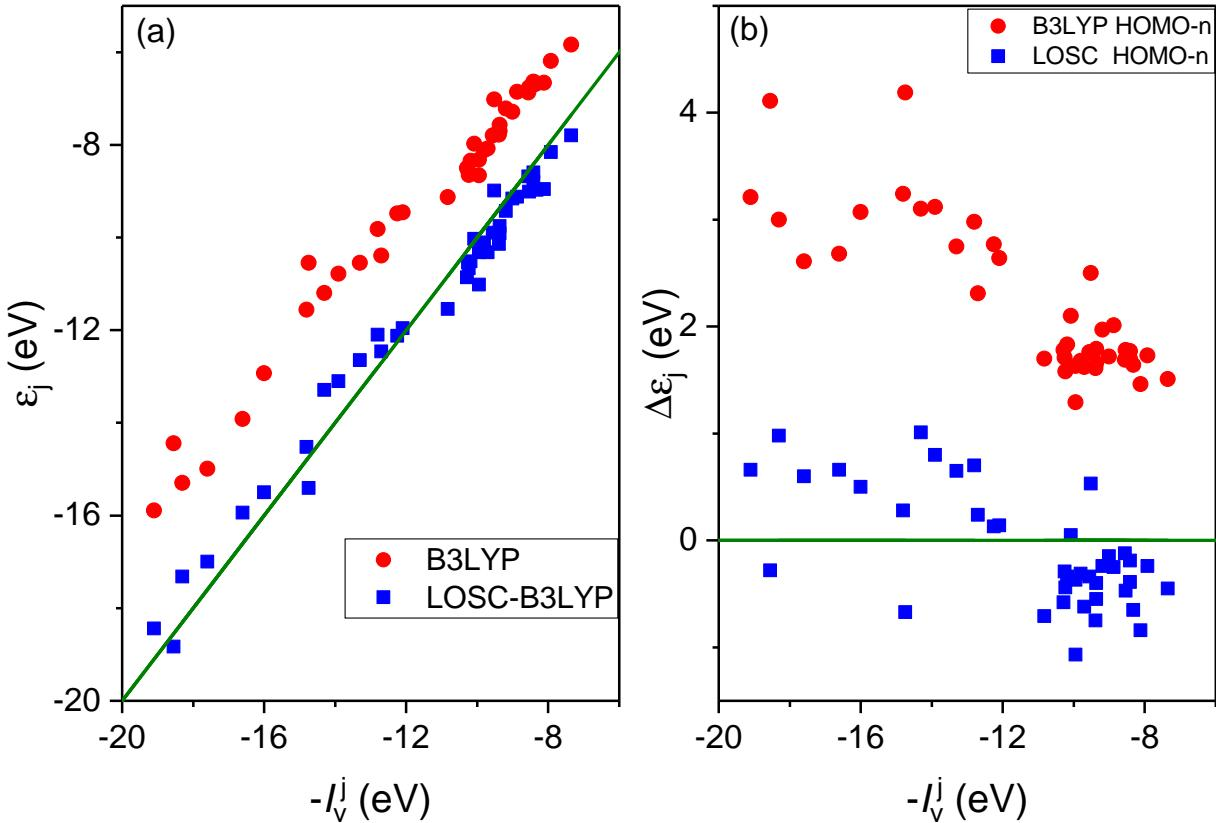


Figure 1: Calculated ε_j of B3LYP and LOSC-B3LYP in comparison with the experimental $-I_v^j$. (a) Orbital energies ε_j for 43 states below HOMO are included. The solid line indicates $\varepsilon_j = -I_v^j$. (b) The errors of calculated orbital energies with respect to the experimental negative VIPs, $\Delta\varepsilon_j = \varepsilon_j + I_v^j$, are recorded.

Besides HOMO and LUMO, Tab. 1 also summarizes the results of valence orbital energies from DFAs and LOSC-DFAs. Similarly, the serious deviation from the experiment by

commonly used DFAs can be largely reduced by L OSC. This can be clearly seen from Fig. 1: valence orbital energies of B3LYP significantly overestimate quasiparticle energies; with L OSC, the systematic error is eliminated. By observing Fig. 1(b), we find that the overestimation of quasiparticle energies by B3LYP becomes more serious for states with lower energies, which is corrected in L OSC-B3LYP.

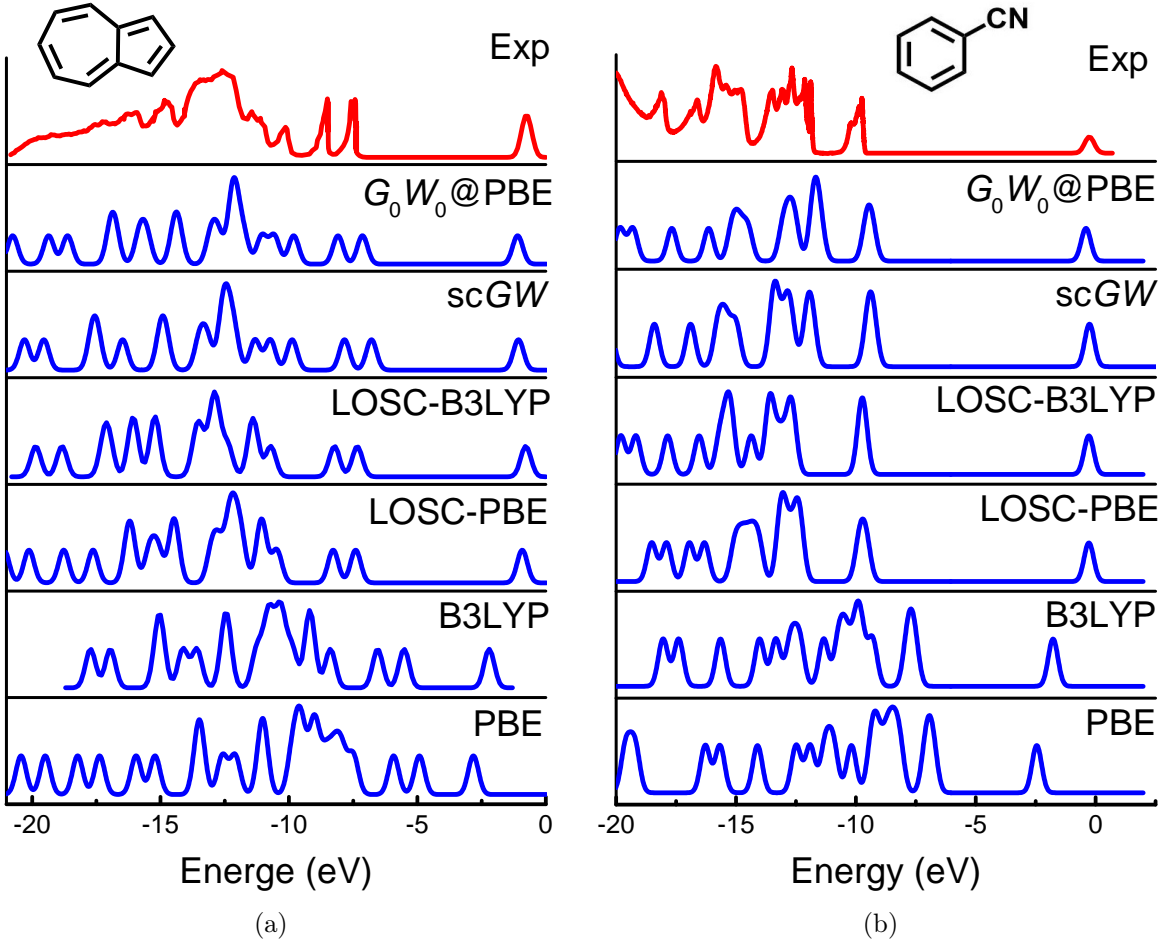


Figure 2: Photoemission spectrum of (a) azulene and (b) benzonitrile. All the calculated spectrum are broadened by Gaussian expansion with 0.2 eV. scGW and G_0W_0 results are obtained from Ref 80. Experimental results are obtained from (a) Ref 88 and (b) Ref 89.

To further confirm that L OSC is a reliable method for the calculation of quasiparticle energies, GKS spectra of forty systems were plotted and compared to the experimental photoemission spectra, along with GW results when available. Fig. 2 only shows the results of azulene and benzonitrile; tests on other molecules give similar results, which can be

found in SI. As can be seen, commonly used DFAs exemplified by PBE and B3LYP give too narrow HOMO-LUMO gaps, with the occupied levels being significantly overestimated and LUMO energy being underestimated. LOSC greatly corrects the results. Furthermore, spectra by LOSC-DFAs are consistent with the experimental photoemission spectra, with the principle peaks appearing at the same positions. Overall, LOSC shows little dependence on parent DFAs, and can reach an accuracy that is comparable to that of GW methods in predicting quasiparticle spectra. Note that the computational cost of LOSC only amounts to a small portion of the parent functional, thus it is computationally much more efficient than G0W0. Therefore, LOSC-DFAs are a promising low-cost alternative to GW approximation for accurate prediction of quasiparticle energies.

Accurate prediction of quasiparticle energies by LOSC-DFAs thus allows the calculation of excitation energies from ground state DFT calculation through Eqs. 2 and 3. Because anionic systems ($(N + 1)$ -electron systems) are generally difficult to converge to right states, here we only discuss the excitation energies calculated from $(N - 1)$ -electron systems; some results from $(N + 1)$ -electron systems can be found in SI. For the excitations of HOMO to orbitals above HOMO, starting from the doublet ground state of $(N - 1)$ -electron systems (assuming one more α -spin electron than β -spin electrons), there are two orbital energies of different spins for each orbital above HOMO. Apparently, α -spin orbital energies should be used for triplet excitations. For singlet excitations, a spin purification process similar to Refs. 60 and ? is used here, and the excitation energies are calculated by

$$\Delta E_m^{\text{singlet}}(N) \approx [2\varepsilon_m^\beta(N - 1) - \varepsilon_m^\alpha(N - 1)] - \varepsilon_{\text{HOMO}}^\beta(N - 1). \quad (4)$$

The results of 48 low-lying excitation energies obtained from different DFAs and LOSC-DFAs are summarized in Tab. 2, where triplet and singlet excitations are categorized and presented. The results from Hartree Fock (HF), TDDFT and Δ SCF-DFT with B3LYP functional are also listed for comparison. As expected, LOSC-DFAs can provides good

Table 2: Mean absolute errors (MAEs, in eV) and mean sign errors (MSEs, in eV) of 48 low-lying excitation energies obtained from HF, DFT, TDDFT and Δ SCF-B3LYP calculation on 16 molecules. Notation T1 refers to triplet HOMO to LUMO excitation, and T2 refers to triplet HOMO to LUMO+1 excitation. The analogy notation for S1 and S2 which stand for singlet excitations. Reference data were obtained from Ref 90.

Method	T1		T2		S1		S2		Total	
	MAE	MSE	MAE	MSE	MAE	MSE	MAE	MSE	MAE	MSE
HF	1.08	-0.88	2.04	-1.23	1.12	-0.59	1.49	0.81	1.35	-0.83
BLYP	0.19	-0.14	0.63	-0.10	0.68	-0.65	0.65	-0.24	0.53	-0.22
B3LYP	0.17	-0.13	0.43	0.01	0.45	-0.33	0.67	-0.58	0.42	-0.01
LDA	0.24	-0.02	0.65	0.04	0.73	-0.68	0.70	-0.27	0.58	-0.16
LOSC-BLYP	0.49	-0.28	0.46	-0.37	0.84	-0.84	0.62	0.10	0.63	-0.44
LOSC-B3LYP	0.30	-0.23	0.28	-0.14	0.60	-0.51	0.69	-0.29	0.49	-0.19
LOSC-LDA	0.48	-0.18	0.52	-0.27	0.88	-0.88	0.71	0.11	0.67	-0.42
TD-B3LYP	0.45	-0.45	0.39	-0.39	0.38	-0.35	0.28	0.27	0.38	-0.37
Δ -SCF	0.20	-0.16	0.33	-0.24	0.56	-0.56	0.18	0.04	0.35	-0.31

prediction for excitation energies due to their excellent performance on quasiparticle energies. Especially, the total MAE and MSE of LOSC-B3LYP are 0.49 eV and -0.19 eV, which are comparable to TDDFT (MAE of 0.38 eV and MSE of -0.37 eV) and Δ SCF-DFT (MAE of 0.35 eV and MSE of -0.31 eV, based on the same reference DFA (B3LYP). For conventional DFAs, it is surprising to find that they have very good performance on predicting low-lying excitation energies, even though they perform poorly in quasiparticle energy calculations. These good results should be attributed to the fact that unoccupied (or occupied) orbitals that are energetically close suffer from a similar amount of systematic delocalization error, making the error cancellation when calculating excitation energies from the difference of orbital energies. This can be seen clearly by comparing their performance on the T1 (HOMO-LUMO excitation) and T2 (HOMO-(LUMO+1) excitation). Conventional DFAs tested here perform very well on T1 excitation (MAEs are around 0.2 eV), but their performance on T2 excitation is much worse (MAEs can be larger than 0.6 eV). In contrast, LOSC-DFAs are consistent in their performance for these two types of excitations. Thus, it can be inferred that for a DFT method to achieve good accuracy for the prediction of excitation energies of

low- to high-lying states, it is necessary to provide consistently reliable quasiparticle energies for all different states involved.

Table 3: Mean absolute errors (MAEs, in eV) and mean sign errors (MSEs, in eV) with respect to experimental reference of excitation energies of 4 atoms from low-lying states to Rydberg states. 12 excitations were included for each atom. Experimental values were obtained from Ref 91.

		LDA	BLYP	B3LYP	LOSC-LDA	LOSC-BLYP	LOSC-B3LYP
Be singlet ^a	MAE	2.37	1.15	1.85	0.24	0.54	0.35
	MSE	2.37	-1.15	1.85	0.07	-0.29	-0.06
Be triplet ^a	MAE	2.30	1.91	1.79	0.28	0.60	0.30
	MSE	2.11	1.68	1.79	-0.04	-0.60	-0.29
Mg singlet ^b	MAE	2.37	2.07	1.69	0.55	0.26	0.21
	MSE	2.37	2.07	1.69	0.55	0.16	0.21
Mg triplet ^b	MAE	2.13	1.82	1.54	0.40	0.15	0.14
	MSE	2.12	1.80	1.52	0.34	-0.11	0.06
Li doublet ^a	MAE	0.97	1.77	1.40	0.91	0.17	0.16
	MSE	0.97	1.77	1.40	-0.89	0.04	-0.03
Na doublet ^b	MAE	1.52	2.16	1.69	0.25	0.57	0.42
	MSE	1.52	2.16	1.69	-0.11	0.57	0.42

^a The excitation states are calculated up to atomic orbital 6p.

^b The excitation states are calculated up to atomic orbital 7p.

To further confirm the above inference, four atoms (Li, Be, Mg, and Na) are selected as an atomic set to test their excitation energies up to Rydberg states. Table 3 summarizes the MAEs from different DFAs and LOSC-DFAs applied to this atomic test set, more detailed results can be found in SI. As can be seen, conventional DFAs show large MAEs for all the four atoms. By observing Tabs. S7 to S12 in SI, it is easy to find that the higher the excited states, the greater the deviation between the results obtained by DFAs and the experimental values. This is because conventional DFAs show larger errors for quasiparticle energies at higher states, thus the difference of orbital energies cannot completely offset the systematic delocalization errors of orbitals that are energetically far apart. In contrast, LOSC-DFAs perform similarly for different excited states with very high accuracy, which should be attributed to the good performance of LOSC on quasiparticle energies of different states.

In conclusion, we have carried out a comprehensive test on calculations of quasiparticle energies and excitation energies with the LOSC functional and DFAs. Through a large number of comparisons with experimental results and GW results, we demonstrated that LOSC-DFAs shows little dependence on parent DFAs, and can reach an accuracy that is better or comparable to that of GW methods in predicting quasiparticle spectra. This also leads to the calculations of excitation energies of the N -electron systems from ground state calculations of the $(N - 1)$ -electron systems. Commonly used DFAs show good performance for valence excitations, but not accurate for higher energy and Rydberg states; in contrast, LOSC-DFAs can provide consistently accurate results for excitation energies from low-lying to Rydberg states. This work highlights the pathway to quasiparticle and excitation energies from ground density functional calculations.

Note. When preparing the manuscript for submission, we became aware of Ref. 92, which also calculated excitation energies from orbital energy differences of the $(N - 1)$ -electron systems. Different functionals from our tests and only valence excitations were reported.

Acknowledgement

Support from the National Institutes of Health (Grant No. R01 GM061870-13) (WY), the Center for Computational Design of Functional Layered Materials (Award DE-SC0012575), an Energy Frontier Research Center funded by the US Department of Energy, Office of Science, Basic Energy Sciences. (YM, NQS), and the National Science Foundation (CHE-1362927) (CL) is appreciated. The authors were grateful to Dr. Noa Marom for providing detailed data from Ref. 80.

Supporting Information Available

The following files are available free of charge.

- SI.pdf: More details of computations and test results.

References

- (1) Fetter, A. L.; Walecka, J. D. *Quantum Theory of Many-Particle Systems*; Dover, New York, 2003.
- (2) Dickhoff, W. H.; Van Neck, D. *Many-Body Theory Exposed!*, 2nd ed.; WORLD SCIENTIFIC, 2008.
- (3) Martin, R. M.; Reining, L.; Ceperley, D. M. *Interacting Electrons: Theory and Computational Approaches*; Cambridge: Cambridge University Press, 2016.
- (4) Hedin, L. New Method for Calculating the One-Particle Green's Function with Application to the Electron-Gas Problem. *Phys. Rev.* **1965**, *139*, A796–A823.
- (5) Aryasetiawan, F.; Gunnarsson, O. The GW method. *Reports on Progress in Physics* **1998**, *61*, 237.
- (6) Onida, G.; Reining, L.; Rubio, A. Electronic excitations: density-functional versus many-body Green's-function approaches. *Rev. Mod. Phys.* **2002**, *74*, 601–659.
- (7) Holm, B.; von Barth, U. Fully self-consistent GW self-energy of the electron gas. *Phys. Rev. B* **1998**, *57*, 2108–2117.
- (8) Hohenberg, P.; Kohn, W. Inhomogeneous electron gas. *Physical review* **1964**, *136*, B864.
- (9) Kohn, W.; Sham, L. J. Self-consistent equations including exchange and correlation effects. *Physical review* **1965**, *140*, A1133.
- (10) Parr, R. G.; Yang, W. *Density-Functional Theory of Atoms and Molecules*; Oxford University Press, New York, 1989.

- (11) Perdew, J. P.; Parr, R. G.; Levy, M.; Balduz, J. L. Density-Functional Theory for Fractional Particle Number - Derivative Discontinuities of the Energy. *Phys. Rev. Lett.* **1982**, *49*, 1691–1694.
- (12) Perdew, J. P.; Levy, M. Physical Content of the Exact Kohn-Sham Orbital Energies - Band-Gaps and Derivative Discontinuities. *Phys. Rev. Lett.* **1983**, *51*, 1884–1887.
- (13) Levy, M.; Perdew, J. P.; Sahni, V. Exact Differential-Equation for the Density and Ionization-Energy of a Many-Particle System. *Phys. Rev. A* **1984**, *30*, 2745–2748.
- (14) Almbladh, C. O.; Pedroza, A. C. Density-functional exchange-correlation potentials and orbital eigenvalues for light atoms. *Phys. Rev. A* **1984**, *29*, 2322–2330.
- (15) Almbladh, C.-O.; von Barth, U. Exact results for the charge and spin densities, exchange-correlation potentials, and density-functional eigenvalues. *Phys. Rev. B* **1985**, *31*, 3231–3244.
- (16) Perdew, J. P.; Levy, M. Comment on "Significance of the highest occupied Kohn-Sham eigenvalue". *Phys. Rev. B* **1997**, *56*, 16021–16028.
- (17) Casida, M. E. Correlated optimized effective-potential treatment of the derivative discontinuity and of the highest occupied Kohn-Sham eigenvalue: A Janak-type theorem for the optimized effective-potential model. *Phys. Rev. B* **1999**, *59*, 4694–4698.
- (18) Cohen, A. J.; Mori-Sánchez, P.; Yang, W. Fractional charge perspective on the band gap in density-functional theory. *Phys. Rev. B* **2008**, *77*, 115123.
- (19) Yang, W.; Cohen, A. J.; Mori-Sánchez, P. Derivative discontinuity, bandgap and lowest unoccupied molecular orbital in density functional theory. *J. Chem. Phys.* **2012**, *136*.
- (20) Zhang, Y. K.; Yang, W. T. Perspective on "Density-functional theory for fractional particle number: derivative discontinuities of the energy" Perdew JP, Parr RG, Levy M, Balduz JL Jr. *Theor. Chem. Acc.* **2000**, *103*, 346–348.

- (21) Yang, W.; Zhang, Y. K.; Ayers, P. W. Degenerate ground states and a fractional number of electrons in density and reduced density matrix functional theory. *Phys. Rev. Lett.* **2000**, *84*, 5172–5175.
- (22) Perdew, J. P.; Ruzsinszky, A.; Csonka, G. I.; Vydrov, O. A.; Scuseria, G. E.; Staroverov, V. N.; Tao, J. Exchange and correlation in open systems of fluctuating electron number. *Phys. Rev. A* **2007**, *76*, 040501.
- (23) Mori-Sánchez, P.; Cohen, A. J.; Yang, W. Localization and delocalization errors in density functional theory and implications for band-gap prediction. *Phys. Rev. Lett.* **2008**, *100*, 146401.
- (24) Chong, D. P.; Gritsenko, O. V.; Baerends, E. J. Interpretation of the KohnâĂŞSham orbital energies as approximate vertical ionization potentials. *J. Chem. Phys.* **2002**, *116*, 1760–1772.
- (25) Gritsenko, O. V.; Braïda, B.; Baerends, E. J. Physical interpretation and evaluation of the KohnâĂŞSham and Dyson components of the ÎtâĂŞI relations between the KohnâĂŞSham orbital energies and the ionization potentials. *J. Chem. Phys.* **2003**, *119*, 1937–1950.
- (26) Bartlett, R. J.; Ranasinghe, D. S. The power of exact conditions in electronic structure theory. *Chem. Phys. Lett.* **2017**, *669*, 54 – 70.
- (27) Ranasinghe, D. S.; Margraf, J. T.; Jin, Y.; Bartlett, R. J. Does the ionization potential condition employed in QTP functionals mitigate the self-interaction error? *J. Chem. Phys.* **2017**, *146*, 034102.
- (28) Bartlett, R. J. Towards an exact correlated orbital theory for electrons. *Chemical Physics Letters* **2009**, *484*, 1 – 9.

- (29) Fuks, J. I.; Maitra, N. T. Challenging adiabatic time-dependent density functional theory with a Hubbard dimer: the case of time-resolved long-range charge transfer. *Phys. Chem. Chem. Phys.* **2014**, *16*, 14504–14513.
- (30) Cohen, A. J.; Mori-Sánchez, P.; Yang, W. Challenges for Density Functional Theory. *Chem. Rev.* **2012**, *112*, 289–320.
- (31) Cohen, A. J.; Mori-Sánchez, P.; Yang, W. Insights into current limitations of density functional theory. *Science* **2008**, *321*, 792–794.
- (32) Cohen, A. J.; Mori-Sánchez, P.; Yang, W. Development of exchange-correlation functionals with minimal many-electron self-interaction error. *J. Chem. Phys.* **2007**, *126*, 191109.
- (33) Gill, P. M. W.; Adamson, R. D.; Pople, J. A. Coulomb-attenuated exchange energy density functionals. *Mol. Phys.* **1996**, *88*, 1005–1009.
- (34) Leininger, T.; Stoll, H.; Werner, H. J.; Savin, A. Combining long-range configuration interaction with short-range density functionals. *Chem. Phys. Lett.* **1997**, *275*, 151–160.
- (35) Iikura, H.; Tsuneda, T.; Yanai, T.; Hirao, K. A long-range correction scheme for generalized-gradient-approximation exchange functionals. *J. Chem. Phys.* **2001**, *115*, 3540–3544.
- (36) Tsuneda, T.; Song, J. W.; Suzuki, S.; Hirao, K. On Koopmans' theorem in density functional theory. *J. Chem. Phys.* **2010**, *133*, 174101.
- (37) Grimme, S. Semiempirical hybrid density functional with perturbative second-order correlation. *J. Chem. Phys.* **2006**, *124*, 034108.
- (38) Zhang, Y.; Xu, X.; Goddard, W. A. Doubly hybrid density functional for accurate descriptions of nonbond interactions, thermochemistry, and thermochemical kinetics. *Proc. Natl. Acad. Sci. U. S. A.* **2009**, *106*, 4963–4968.

- (39) Su, N.; Yang, W.; Mori-Sánchez, P.; Xu, X. Fractional charge behavior and band gap predictions with the XYG3 type of doubly hybrid density functionals. *J. Phys. Chem. A* **2014**, *118*, 9201–9211.
- (40) Baer, R.; Livshits, E.; Salzner, U. Tuned Range-Separated Hybrids in Density Functional Theory. *Annu. Rev. Phys. Chem.* **2010**, *61*, 85–109.
- (41) Stein, T.; Eisenberg, H.; Kronik, L.; Baer, R. Fundamental Gaps in Finite Systems from Eigenvalues of a Generalized Kohn-Sham Method. *Phys. Rev. Lett.* **2010**, *105*, 266802.
- (42) Li, C.; Zheng, X.; Su, N. Q.; Yang, W. Localized orbital scaling correction for systematic elimination of delocalization error in density functional approximations. *Nati. Sci. Rev.* **2018**, *5*, 203–215.
- (43) Emrich, K. An extension of the coupled cluster formalism to excited states (I). *Nuclear Physics A* **1981**, *351*, 379–396.
- (44) Sekino, H.; Bartlett, R. J. A linear response, coupled-cluster theory for excitation energy. *International Journal of Quantum Chemistry* **1984**, *26*, 255–265.
- (45) Geertsen, J.; Rittby, M.; Bartlett, R. J. The equation-of-motion coupled-cluster method: Excitation energies of Be and CO. *Chemical Physics Letters* **1989**, *164*, 57–62.
- (46) Monkhorst, H. J. Calculation of properties with the coupled-cluster method. *International Journal of Quantum Chemistry* **1977**, *12*, 421–432.
- (47) Monkhorst, H.; Dalgaard, E. J. Quantum Chem. Symp., 11 (1977). *Phys. Rev., A* **1983**, *28*, 1217.
- (48) Koch, H.; Christiansen, O.; Jørgensen, P.; Olsen, J. Excitation energies of BH, CH₂ and Ne in full configuration interaction and the hierarchy CCS, CC2, CCSD and CC3 of coupled cluster models. *Chemical physics letters* **1995**, *244*, 75–82.

- (49) Christiansen, O.; Gauss, J.; Schimmelpfennig, B. Spin-orbit coupling constants from coupled-cluster response theory. *Physical Chemistry Chemical Physics* **2000**, *2*, 965–971.
- (50) Helgaker, T.; Jorgensen, P.; Olsen, J. *Molecular electronic-structure theory*; John Wiley & Sons, 2014.
- (51) Buenker, R. J.; Peyerimhoff, S. D. CI method for the study of general molecular potentials. *Theoretica chimica acta* **1968**, *12*, 183–199.
- (52) Potts, D. M.; Taylor, C. M.; Chaudhuri, R. K.; Freed, K. F. The improved virtual orbital-complete active space configuration interaction method, a £packageable£ efficient ab initio many-body method for describing electronically excited states. *The Journal of Chemical Physics* **2001**, *114*, 2592–2600.
- (53) Abrams, M. L.; Sherrill, C. D. Natural orbitals as substitutes for optimized orbitals in complete active space wavefunctions. *Chemical physics letters* **2004**, *395*, 227–232.
- (54) Slavíček, P.; Martínez, T. J. Ab initio floating occupation molecular orbital-complete active space configuration interaction: An efficient approximation to CASSCF. *The Journal of chemical physics* **2010**, *132*, 234102.
- (55) Andersson, K.; Malmqvist, P. A.; Roos, B. O.; Sadlej, A. J.; Wolinski, K. Second-order perturbation theory with a CASSCF reference function. *Journal of Physical Chemistry* **1990**, *94*, 5483–5488.
- (56) Andersson, K.; Malmqvist, P.-Å.; Roos, B. O. Second-order perturbation theory with a complete active space self-consistent field reference function. *The Journal of chemical physics* **1992**, *96*, 1218–1226.
- (57) Bene, J. E. D.; Ditchfield, R.; Pople, J. Self-Consistent Molecular Orbital Methods. X.

Molecular Orbital Studies of Excited States with Minimal and Extended Basis Sets.
The Journal of Chemical Physics **1971**, *55*, 2236–2241.

- (58) Dreuw, A.; Head-Gordon, M. Single-reference ab initio methods for the calculation of excited states of large molecules. *Chemical reviews* **2005**, *105*, 4009–4037.
- (59) Runge, E.; Gross, E. K. Density-functional theory for time-dependent systems. *Physical Review Letters* **1984**, *52*, 997.
- (60) Ziegler, T.; Rauk, A.; Baerends, E. J. On the calculation of multiplet energies by the Hartree-Fock-Slater method. *Theoretica chimica acta* **1977**, *43*, 261–271.
- (61) Laurent, A. D.; Jacquemin, D. TD-DFT benchmarks: A review. *International Journal of Quantum Chemistry* **2013**, *113*, 2019–2039.
- (62) Tozer, D. J.; Handy, N. C. On the determination of excitation energies using density functional theory. *Physical Chemistry Chemical Physics* **2000**, *2*, 2117–2121.
- (63) Liu, T.; Han, W.-G.; Himo, F.; Ullmann, G. M.; Bashford, D.; Toutchkine, A.; Hahn, K. M.; Noddleman, L. Density functional vertical self-consistent reaction field theory for solvatochromism studies of solvent-sensitive dyes. *The Journal of Physical Chemistry A* **2004**, *108*, 3545–3555.
- (64) Ceresoli, D.; Tosatti, E.; Scandolo, S.; Santoro, G.; Serra, S. Trapping of excitons at chemical defects in polyethylene. *The Journal of chemical physics* **2004**, *121*, 6478–6484.
- (65) Cheng, C.-L.; Wu, Q.; Van Voorhis, T. Rydberg energies using excited state density functional theory. *The Journal of chemical physics* **2008**, *129*, 124112.
- (66) Gavnholt, J.; Olsen, T.; Engelund, M.; Schiøtz, J. Δ self-consistent field method to obtain potential energy surfaces of excited molecules on surfaces. *Physical Review B* **2008**, *78*, 075441.

- (67) Besley, N. A.; Gilbert, A. T.; Gill, P. M. Self-consistent-field calculations of core excited states. *The Journal of chemical physics* **2009**, *130*, 124308.
- (68) Kowalczyk, T.; Yost, S. R.; Voorhis, T. V. Assessment of the \hat{T} TSCF density functional theory approach for electronic excitations in organic dyes. *The Journal of Chemical Physics* **2011**, *134*, 054128.
- (69) Becke, A. D. Vertical excitation energies from the adiabatic connection. *The Journal of chemical physics* **2016**, *145*, 194107.
- (70) Maitra, N. T.; Zhang, F.; Cave, R. J.; Burke, K. Double excitations within time-dependent density functional theory linear response. *The Journal of chemical physics* **2004**, *120*, 5932–5937.
- (71) Levine, B. G.; Ko, C.; Quenneville, J.; MartÍnez, T. J. Conical intersections and double excitations in time-dependent density functional theory. *Molecular Physics* **2006**, *104*, 1039–1051.
- (72) Tozer, D. J.; Handy, N. C. Improving virtual Kohn–Sham orbitals and eigenvalues: Application to excitation energies and static polarizabilities. *The Journal of chemical physics* **1998**, *109*, 10180–10189.
- (73) Casida, M. E.; Jamorski, C.; Casida, K. C.; Salahub, D. R. Molecular excitation energies to high-lying bound states from time-dependent density-functional response theory: Characterization and correction of the time-dependent local density approximation ionization threshold. *The Journal of chemical physics* **1998**, *108*, 4439–4449.
- (74) Casida, M. E.; Salahub, D. R. Asymptotic correction approach to improving approximate exchange–correlation potentials: Time-dependent density-functional theory calculations of molecular excitation spectra. *The Journal of Chemical Physics* **2000**, *113*, 8918–8935.

- (75) Tozer, D. J.; Handy, N. C. The importance of the asymptotic exchange-correlation potential in density functional theory. *Molecular Physics* **2003**, *101*, 2669–2675.
- (76) Tozer, D. J.; Amos, R. D.; Handy, N. C.; Roos, B. O.; Serrano-Andrés, L. Does density functional theory contribute to the understanding of excited states of unsaturated organic compounds? *Molecular physics* **1999**, *97*, 859–868.
- (77) Dreuw, A.; Weisman, J. L.; Head-Gordon, M. Long-range charge-transfer excited states in time-dependent density functional theory require non-local exchange. *The Journal of chemical physics* **2003**, *119*, 2943–2946.
- (78) Dreuw, A.; Head-Gordon, M. Failure of time-dependent density functional theory for long-range charge-transfer excited states: the zincbacteriochlorin- bacteriochlorin and bacteriochlorophyll- spheroidene complexes. *Journal of the American Chemical Society* **2004**, *126*, 4007–4016.
- (79) Blase, X.; Attaccalite, C.; Olevano, V. First-principles GW calculations for fullerenes, porphyrins, phtalocyanine, and other molecules of interest for organic photovoltaic applications. *Physical Review B* **2011**, *83*, 115103.
- (80) Knight, J. W.; Wang, X.; Gallandi, L.; Dolgounitcheva, O.; Ren, X.; Ortiz, J. V.; Rinke, P.; Körzdörfer, T.; Marom, N. Accurate Ionization Potentials and Electron Affinities of Acceptor Molecules III: A Benchmark of GW Methods. *Journal of Chemical Theory and Computation* **2016**, *12*, 615–626, PMID: 26731609.
- (81) An in-house program for QM/MM simulations (<http://www.qm4d.info>).
- (82) Slater, J. C. *The self-consistent field for molecules and solids*; McGraw-Hill New York, 1974; Vol. 4.
- (83) Vosko, S. H.; Wilk, L.; Nusair, M. Accurate spin-dependent electron liquid correlation

- energies for local spin density calculations: a critical analysis. *Canadian Journal of physics* **1980**, *58*, 1200–1211.
- (84) Perdew, J. P.; Burke, K.; Ernzerhof, M. Generalized gradient approximation made simple. *Physical review letters* **1996**, *77*, 3865.
- (85) Becke, A. D. Density-functional exchange-energy approximation with correct asymptotic behavior. *Physical review A* **1988**, *38*, 3098.
- (86) Lee, C.; Yang, W.; Parr, R. G. Development of the Colle-Salvetti correlation-energy formula into a functional of the electron density. *Physical review B* **1988**, *37*, 785.
- (87) Becke, A. D. BeckeâŽs three parameter hybrid method using the LYP correlation functional. *J. Chem. Phys* **1993**, *98*, 5648–5652.
- (88) Dougherty, D.; Lewis, J.; Nauman, R.; McGlynn, S. Photoelectron spectroscopy of azulenes. *Journal of Electron Spectroscopy and Related Phenomena* **1980**, *19*, 21–33.
- (89) Kimura, K. *Handbook of HeI photoelectron spectra of fundamental organic molecules*; Halsted Press, 1981.
- (90) Schreiber, M.; Silva-Junior, M. R.; Sauer, S. P.; Thiel, W. Benchmarks for electronically excited states: CASPT2, CC2, CCSD, and CC3. *The Journal of chemical physics* **2008**, *128*, 134110.
- (91) Kramida, A.; Yu. Ralchenko,; Reader, J.; and NIST ASD Team, NIST Atomic Spectra Database (ver. 5.3), [Online]. Available: <http://physics.nist.gov/asd> [2017, September 3]. National Institute of Standards and Technology, Gaithersburg, MD., 2015.
- (92) Haiduke, R. L. A.; Bartlett, R. J. Communication: Can excitation energies be obtained from orbital energies in a correlated orbital theory? *The Journal of Chemical Physics* **2018**, *149*, 131101.

Supporting information for: Approximating Quasiparticle and Excitation Energies from Ground State Generalized Kohn-Sham Calculations

Yuncai Mei, Chen Li, Neil Qiang Su and Weitao Yang*

Department of Chemistry, Duke University, Durham, North Carolina 27708, USA

E-mail: weitao.yang@duke.edu

Description of LOSC calculation

If not specified, the LOSC calculation in this paper is carried out as a post self-consistent (post-SCF) correction to the parent functional results. In particular, we first perform conventional DFT calculations with the parent functional to obtain the canonical orbitals $\{\varphi_i\}$ and the orbital energies $\{\epsilon_i\}$. Then with the restrained Boys localization (see Ref S1 for details), we obtain the localized orbitals $\{\phi_i\}$. Finally the energy correction and orbital energy corrections are given by

$$\Delta E^{\text{LOSC}} = \sum_{ij} \frac{1}{2} \kappa_{ij} \lambda_{ij} (\delta_{ij} - \lambda_{ij}), \quad (1)$$

and

$$\Delta \epsilon_i = \sum_j \kappa_{jj} \left(\frac{1}{2} - \lambda_{jj} \right) |U_{ji}|^2 - \sum_{j \neq l} \kappa_{jl} \lambda_{jl} U_{ji} U_{li}^*. \quad (2)$$

One can also perform self-consistent field (SCF) calculation for the LOSC, however, it has been demonstrated in Ref S1 that for small and compact molecules, the SCF only slightly differs from the post-SCF results, especially for the orbital energy calculations. So in this paper, we stick with the post-SCF calculations, which is computationally more efficient without much sacrifice in the accuracy of the results. The double integrals in the curvature formula have been evaluated using the resolution of identity (or density fitting) technique.^{S2,S3}

Photoemission spectrum

Figure S1 - S40 show the photoemission spectrum (PES) of 40 test molecules. Most the test molecules were from Blase's^{S4} and Marom's^{S5} test set. In addition, polyacene ($n = 1$ -6) and two big systems (C_{60} and C_{70}) were studied as well for interest. Experimental PES were reproduced from literature as reference, if they were applicable. Experimental electron affinity (see clarification of Table S2 for the data source) was broadened with Gaussian expansion with 0.2 eV to plot a peak in the experimental spectrum. Quasi-particle energies from sc GW and G_0W_0 @PBE were obtained from Ref S5 for Marom's test set and used to plot PES for comparison. For orbital energies from DFT, conventional functional (B3LYP and PBE) and LOSC functional (LOSC-B3LYP and LOSC-PBE) were applied for calculation. cc-pVTZ were used as basis set, if not specified. To obtain PES from GW and DFT, the orbital energies were used and broadened with Gaussian expansion by 0.2 eV for all the test cases.

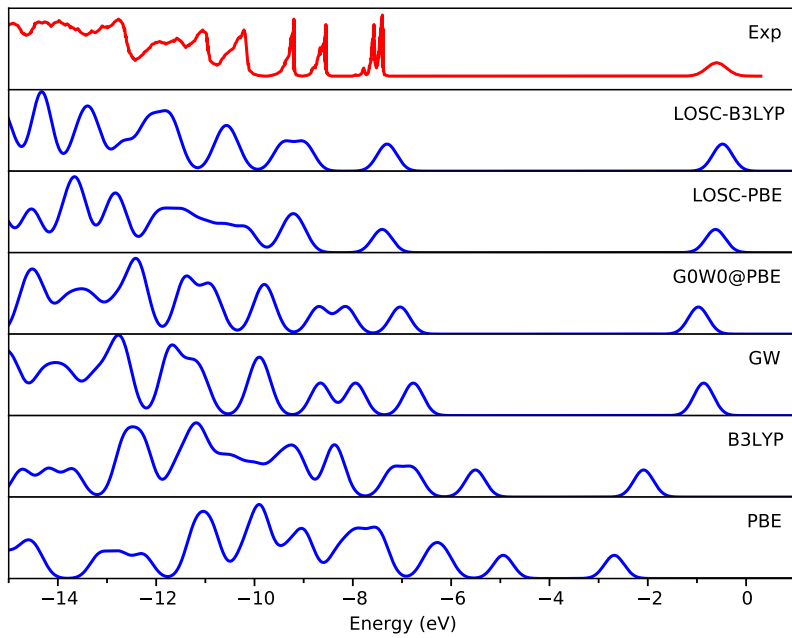


Figure S1: Photoemission spectrum of anthracene. Experimental spectrum was obtained from Ref S6

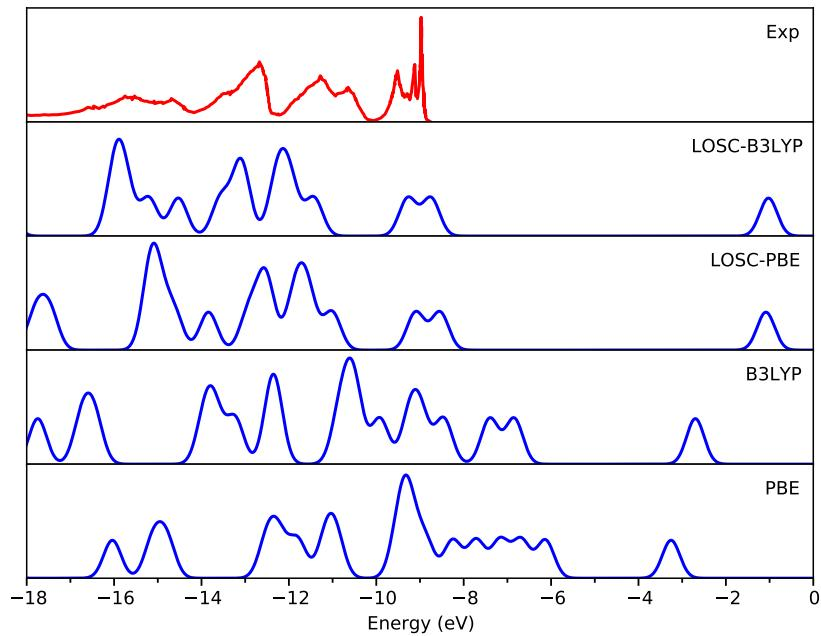


Figure S2: Photoemission spectrum of benzothiadiazole. Experimental spectrum was obtained from Ref S7

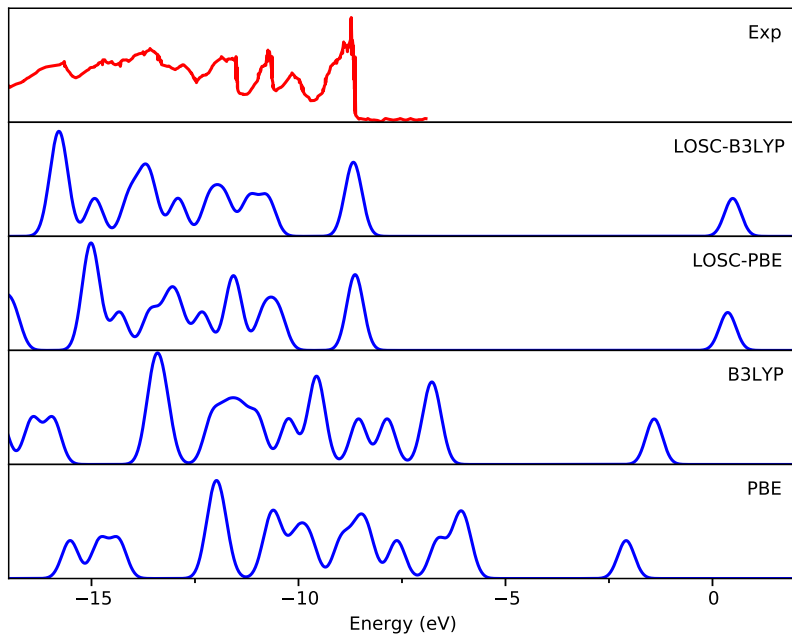


Figure S3: Photoemission spectrum of benzothiazole. Experimental spectrum was obtained from Ref S8

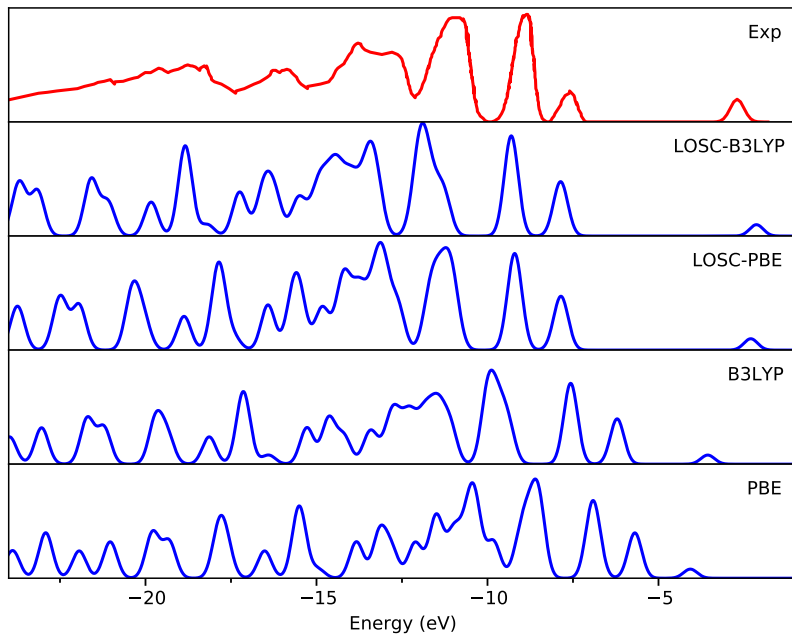


Figure S4: Photoemission spectrum of C_{60} . Experimental spectrum was obtained from Ref S9

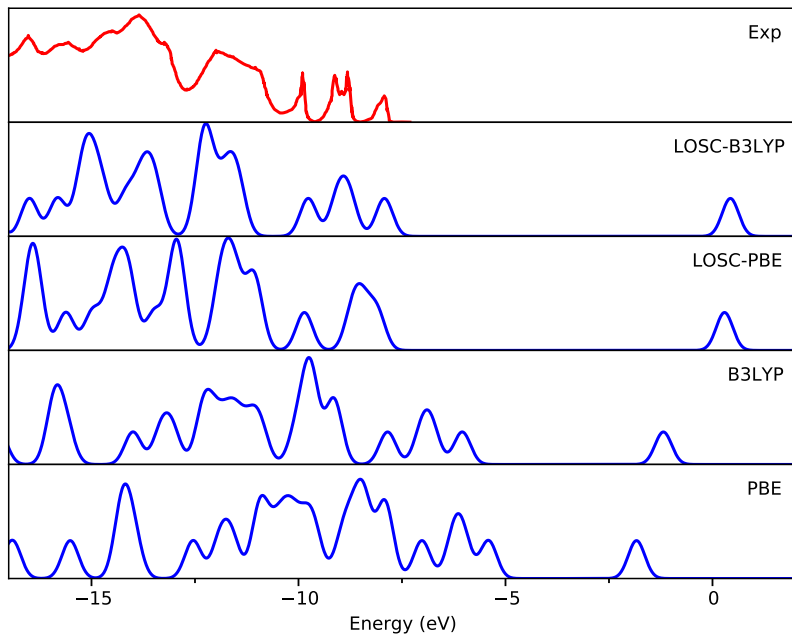


Figure S5: Photoemission spectrum of fluorene. Experimental spectrum was obtained from Ref S10

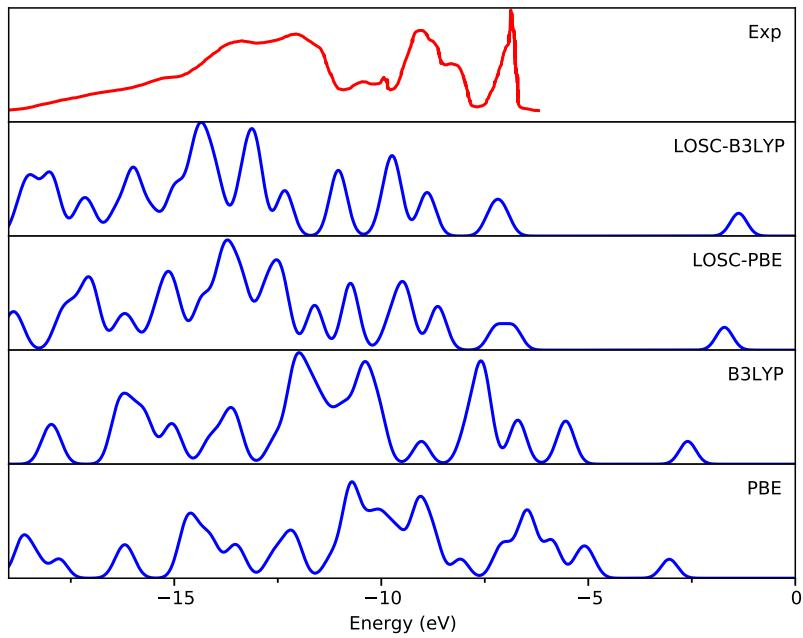


Figure S6: Photoemission spectrum of H_2P . Experimental spectrum was obtained from Ref S11

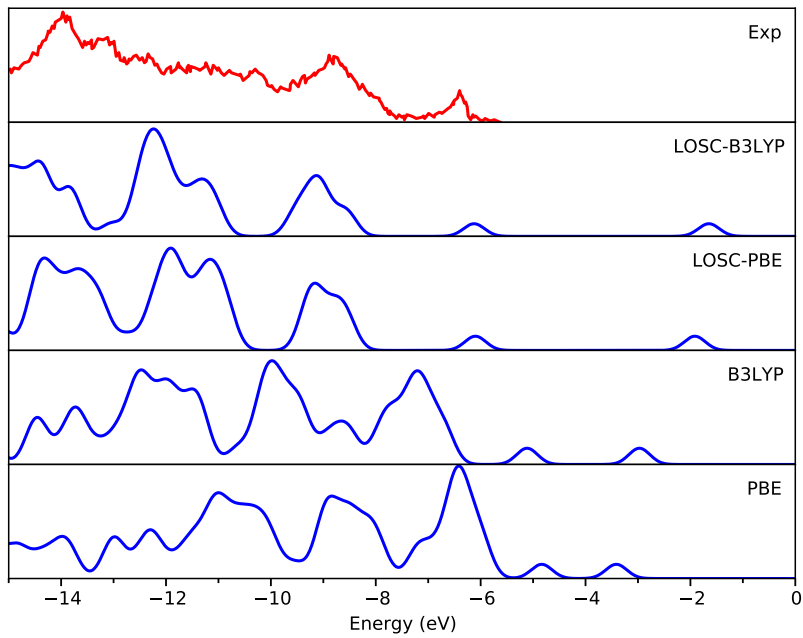


Figure S7: Photoemission spectrum of H_2PC . Experimental spectrum was obtained from Ref S12

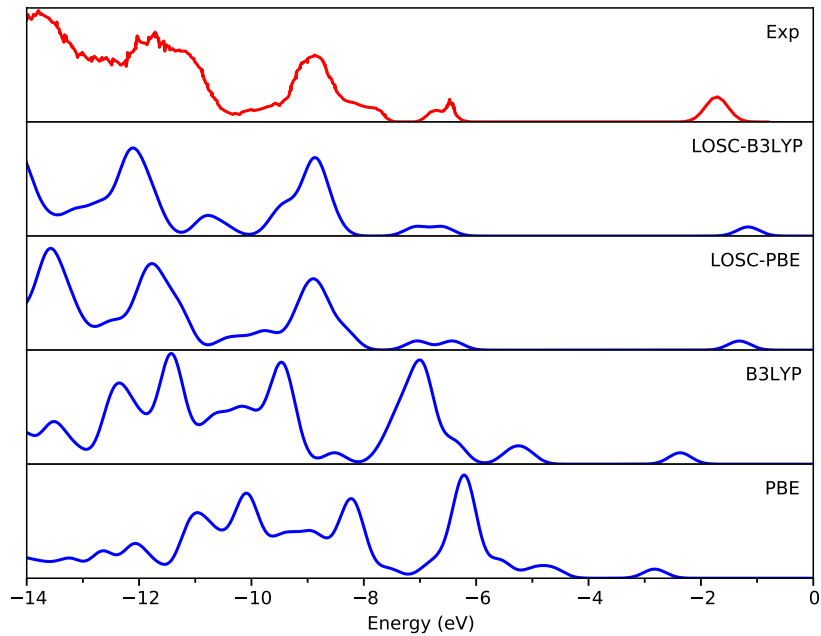


Figure S8: Photoemission spectrum of H_2TPP . Experimental spectrum was obtained from Ref S13

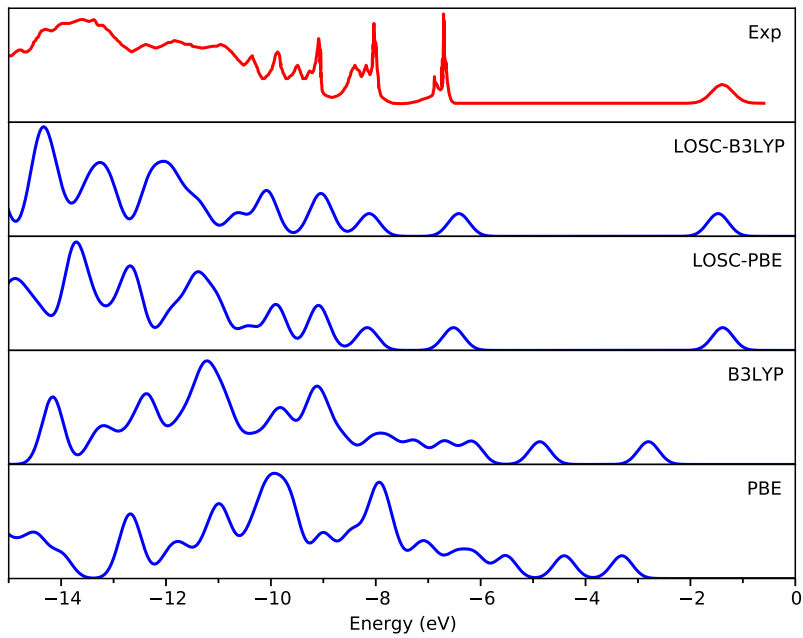


Figure S9: Photoemission spectrum of pentacene. Experimental spectrum was obtained from Ref S14

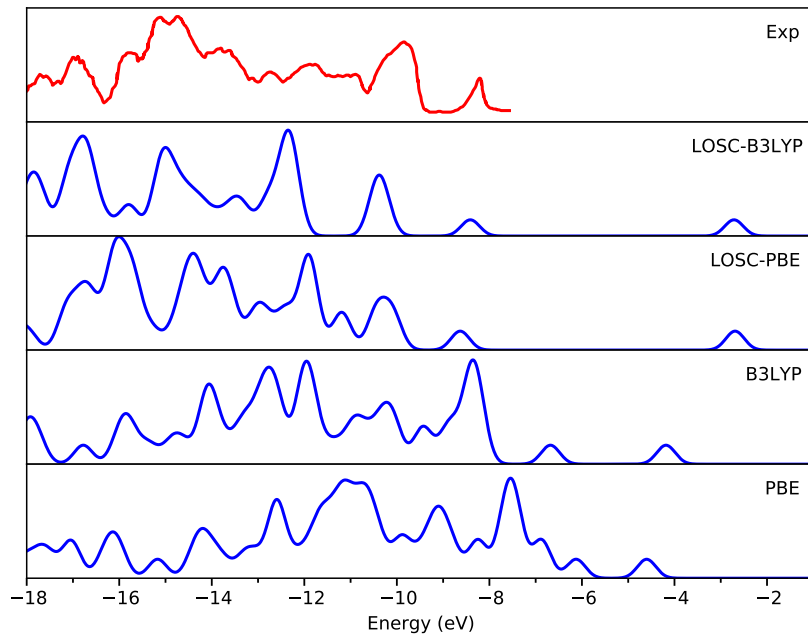


Figure S10: Photoemission spectrum of PTCDA. Experimental spectrum was obtained from Ref S15

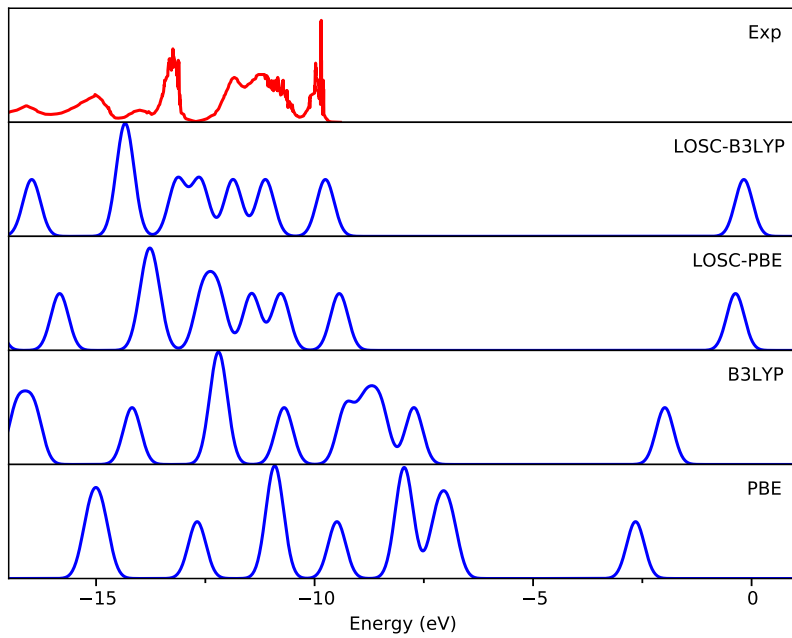


Figure S11: Photoemission spectrum of thiadiazole. Experimental spectrum was obtained from Ref S16

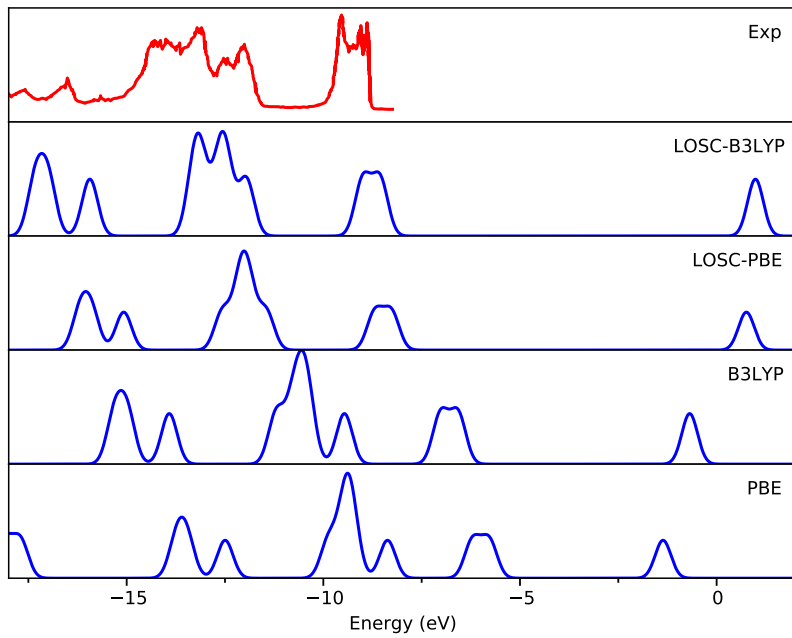


Figure S12: Photoemission spectrum of thiphene. Experimental spectrum was obtained from Ref S17

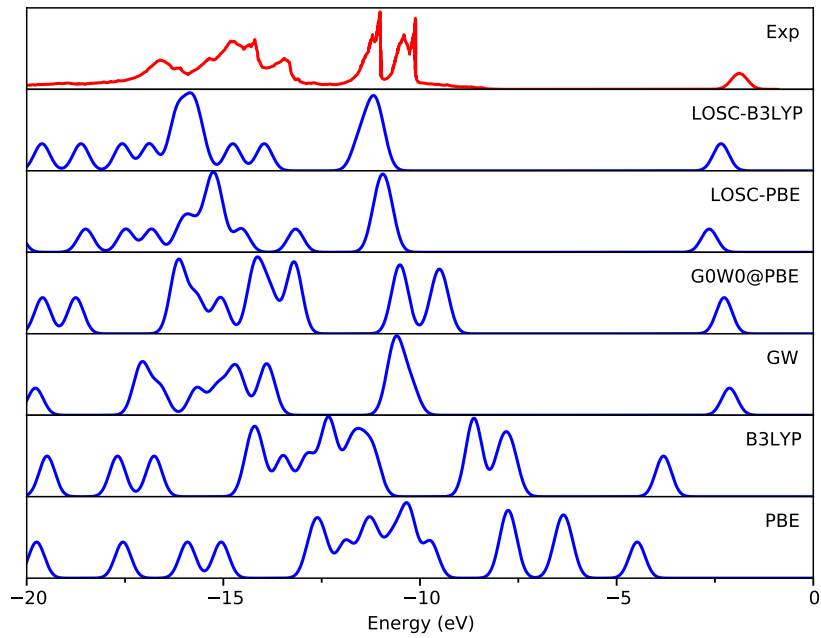


Figure S13: Photoemission spectrum of benzoquinone. Experimental spectrum was obtained from Ref S18

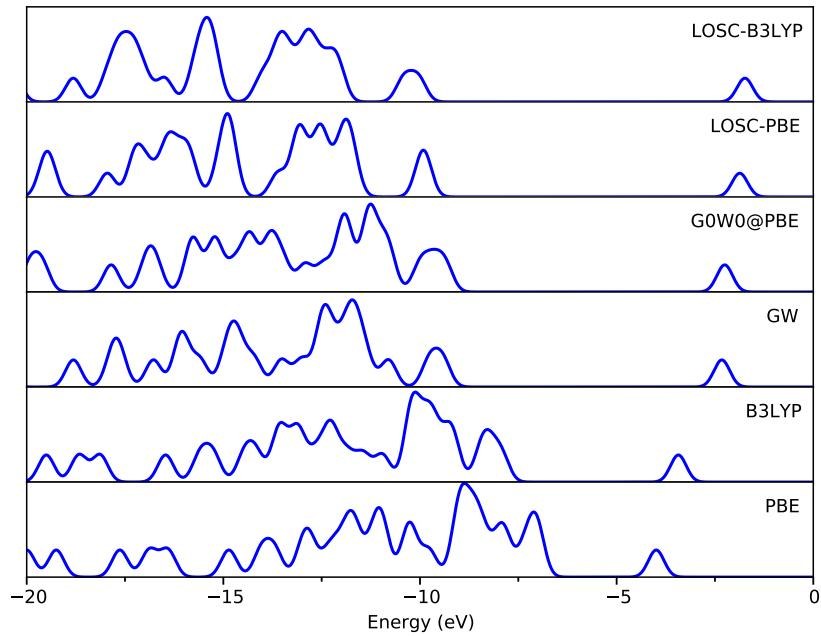


Figure S14: Photoemission spectrum of Cl₄-isobenzofuranedione.

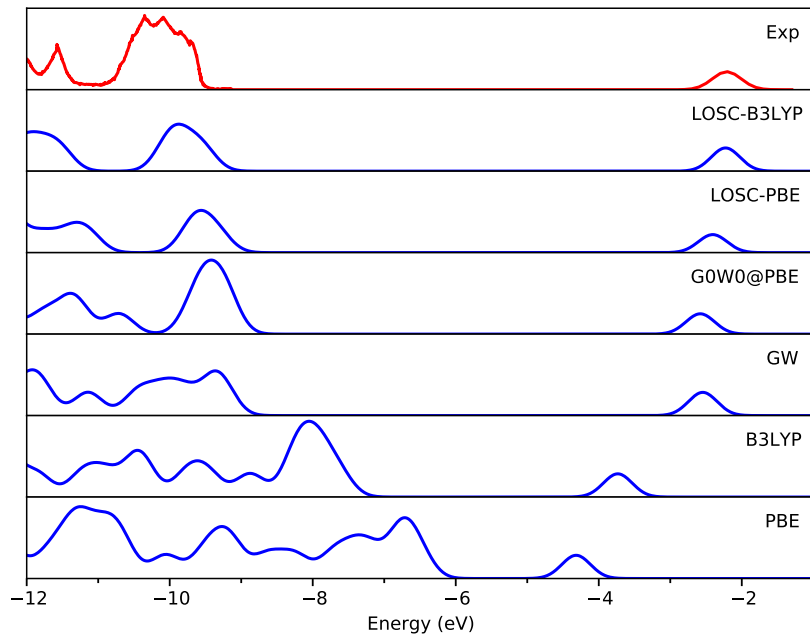


Figure S15: Photoemission spectrum of dichlorone. Experimental spectrum was obtained from Ref S19

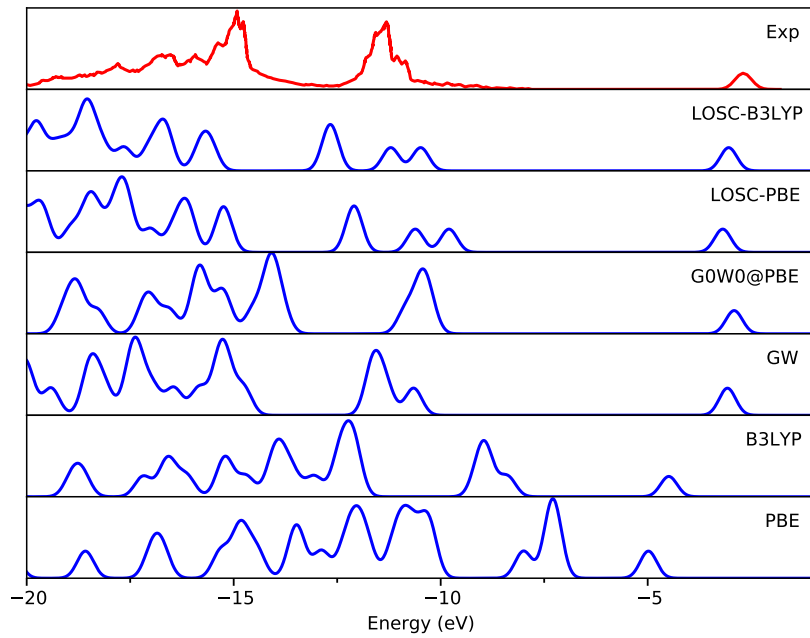


Figure S16: Photoemission spectrum of F_4 -benzoquinone. Experimental spectrum was obtained from Ref S18

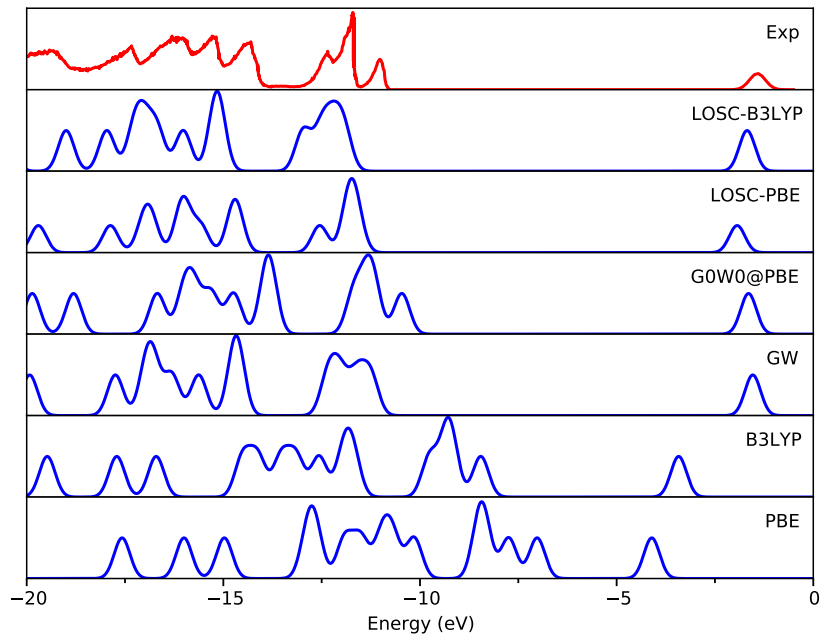


Figure S17: Photoemission spectrum of maleic anhydride. Experimental spectrum was obtained from Ref S5

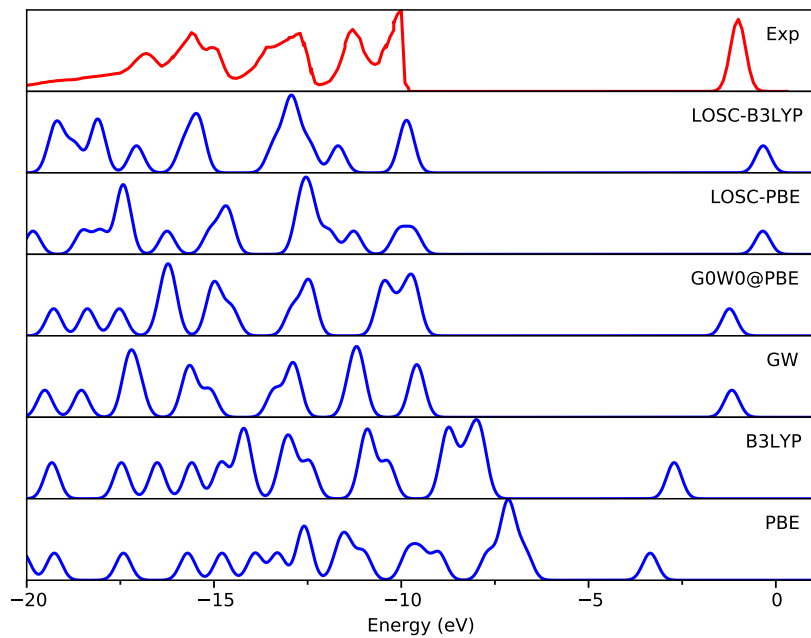


Figure S18: Photoemission spectrum of nitrobenzene. Experimental spectrum was obtained from Ref S20

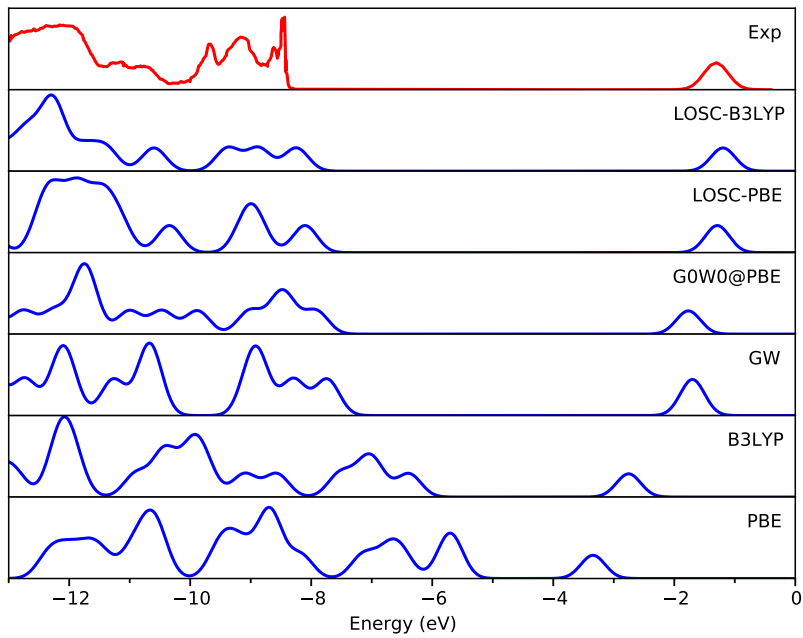


Figure S19: Photoemission spectrum of phenazine. Experimental spectrum was obtained from Ref S21

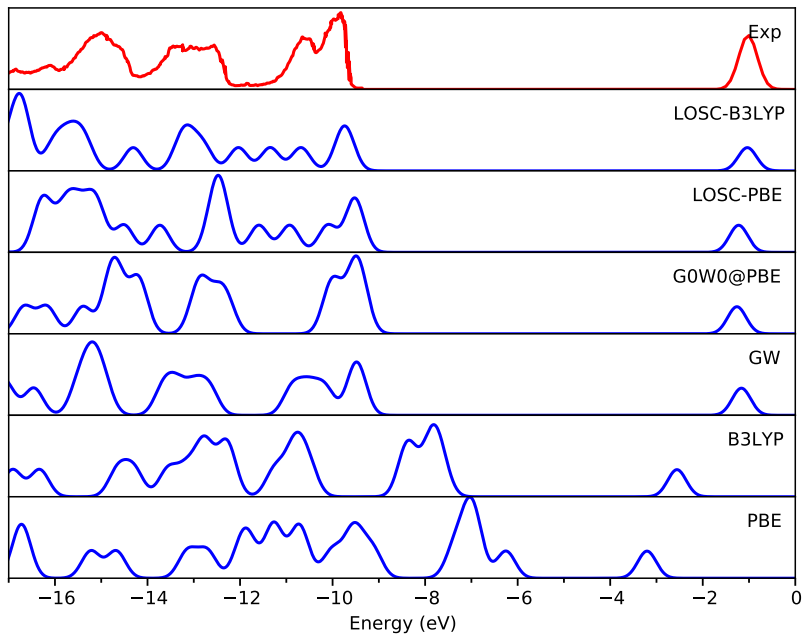


Figure S20: Photoemission spectrum of phthalimide. Experimental spectrum was obtained from Ref S22

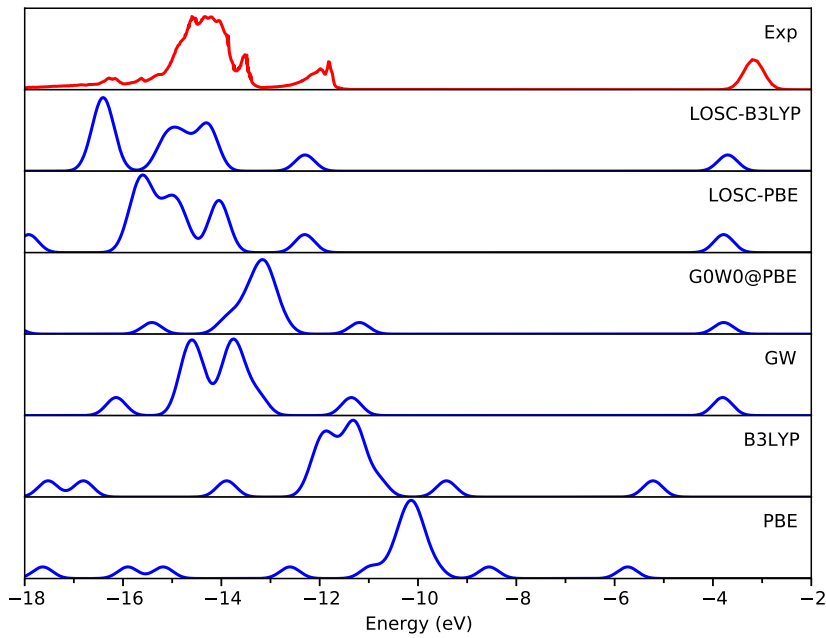


Figure S21: Photoemission spectrum of TCNE. Experimental spectrum was obtained from Ref S23

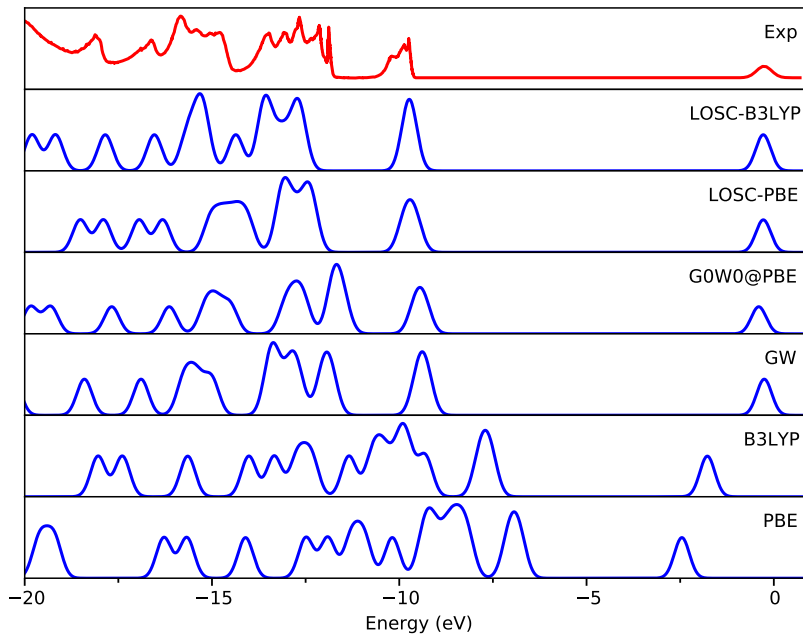


Figure S22: Photoemission spectrum of benzonitrile. Experimental spectrum was obtained from Ref S19

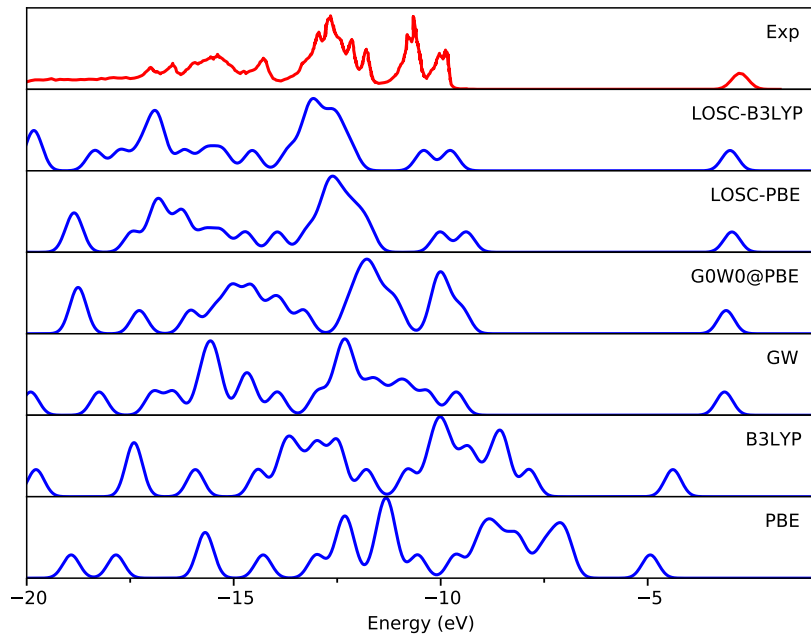


Figure S23: Photoemission spectrum of $\text{Cl}_4\text{-benzoquinone}$. Experimental spectrum was obtained from Ref S24

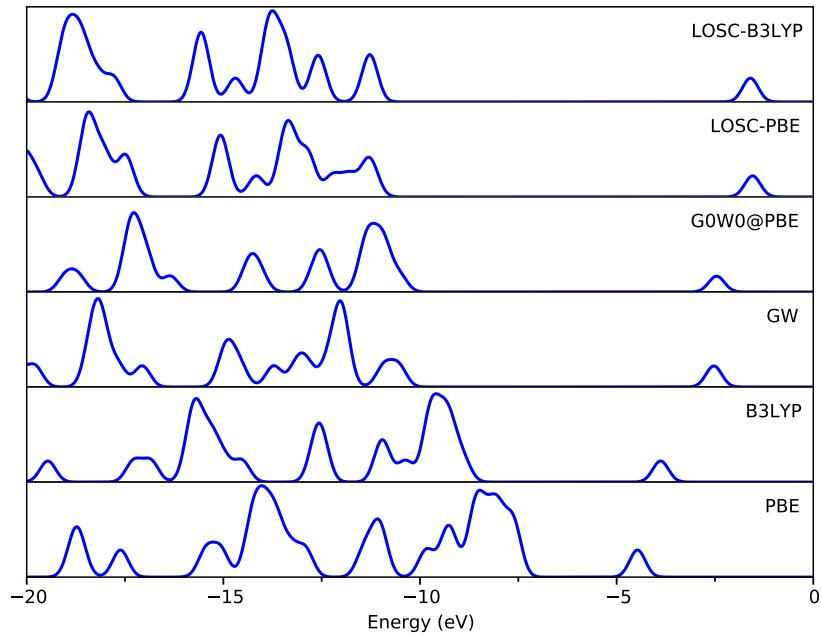


Figure S24: Photoemission spectrum of dinitrobenzonitrile.

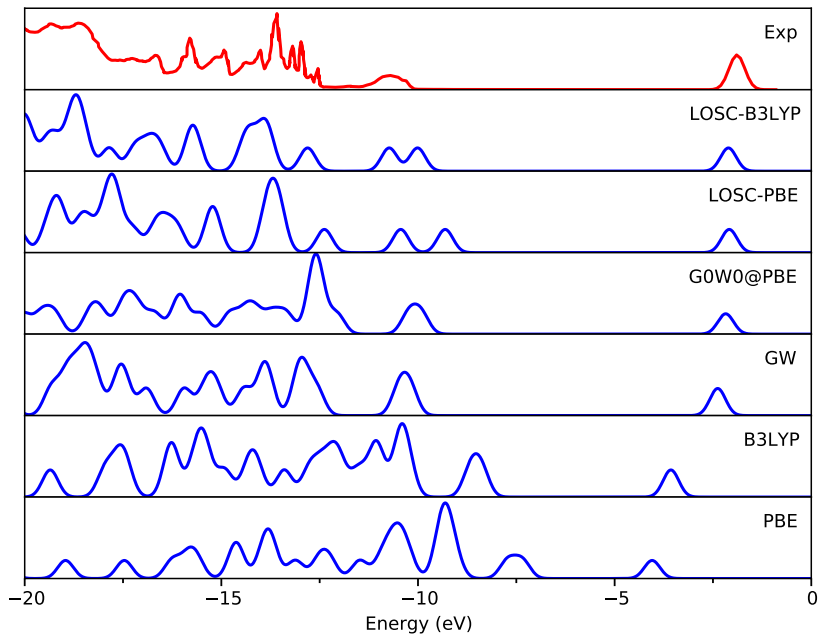


Figure S25: Photoemission spectrum of F_4 -benzenedicarbonitrile. Experimental spectrum was obtained from Ref S25

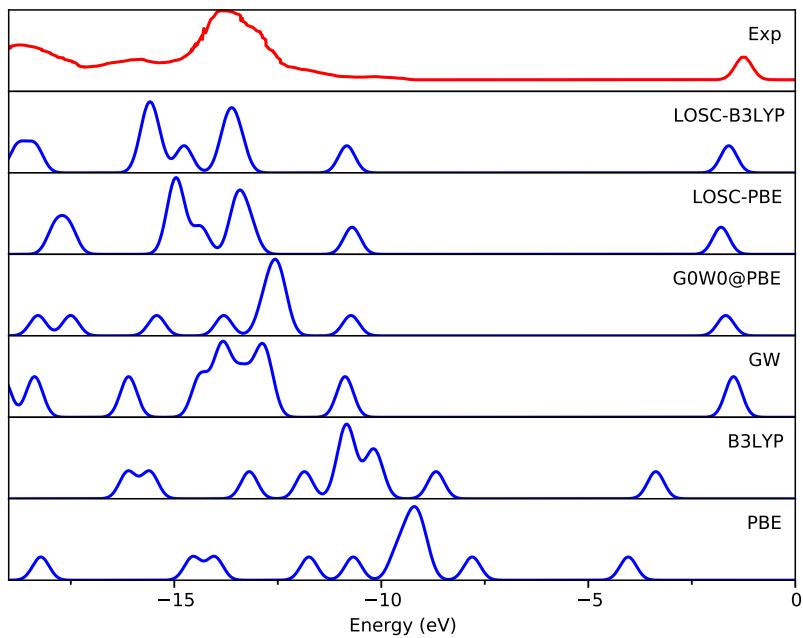


Figure S26: Photoemission spectrum of fumaronitrile. Experimental spectrum was obtained from Ref S26

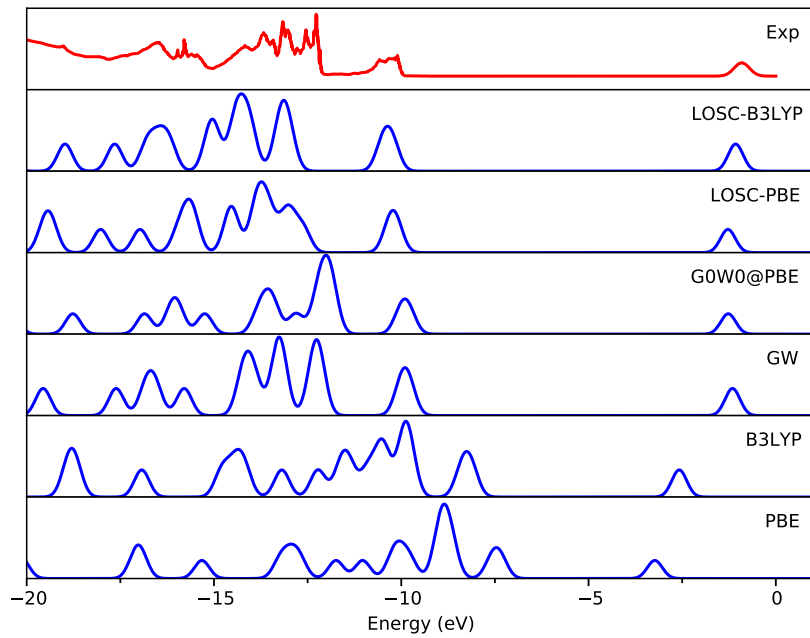


Figure S27: Photoemission spectrum of mDCNB. Experimental spectrum was obtained from Ref S25

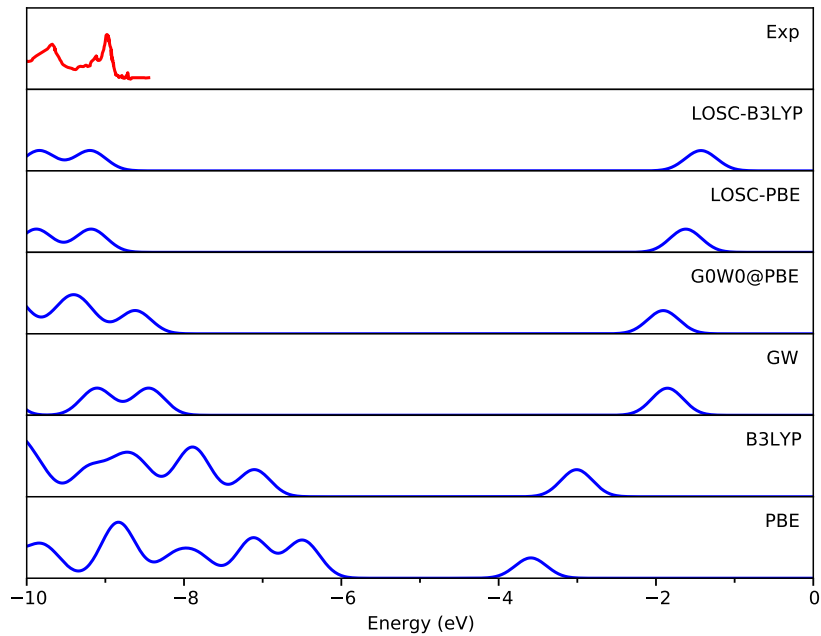


Figure S28: Photoemission spectrum of NDCA. Experimental spectrum was obtained from Ref S27

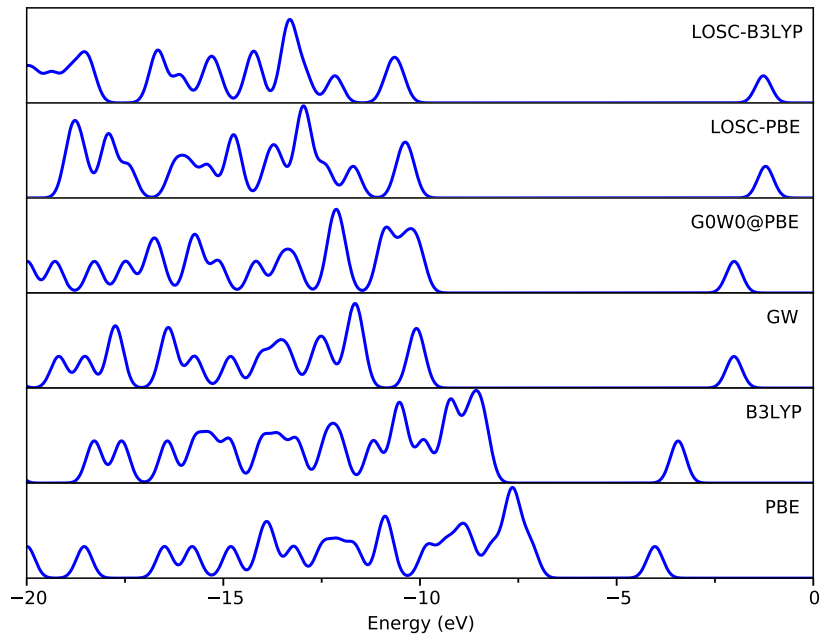


Figure S29: Photoemission spectrum of nitrobenzonitrile.

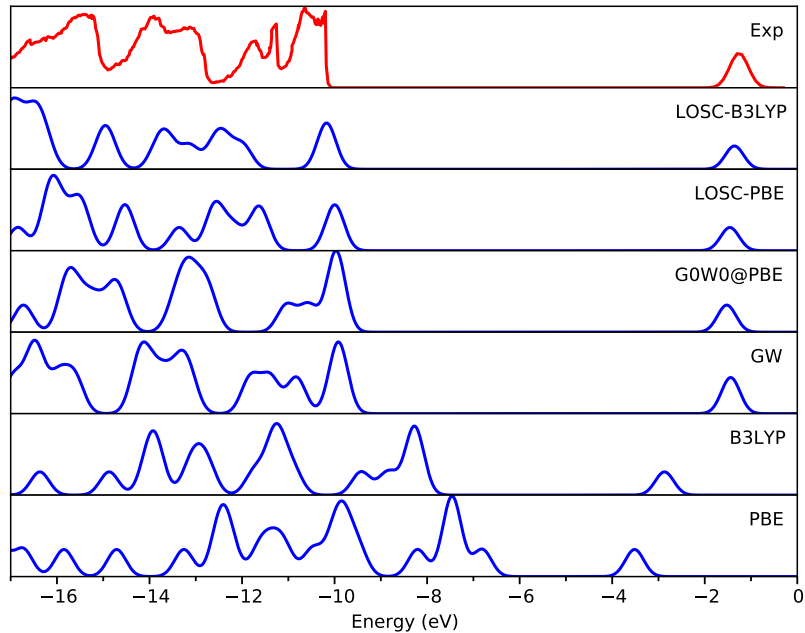


Figure S30: Photoemission spectrum of phthalic anhydride. Experimental spectrum was obtained from Ref S22

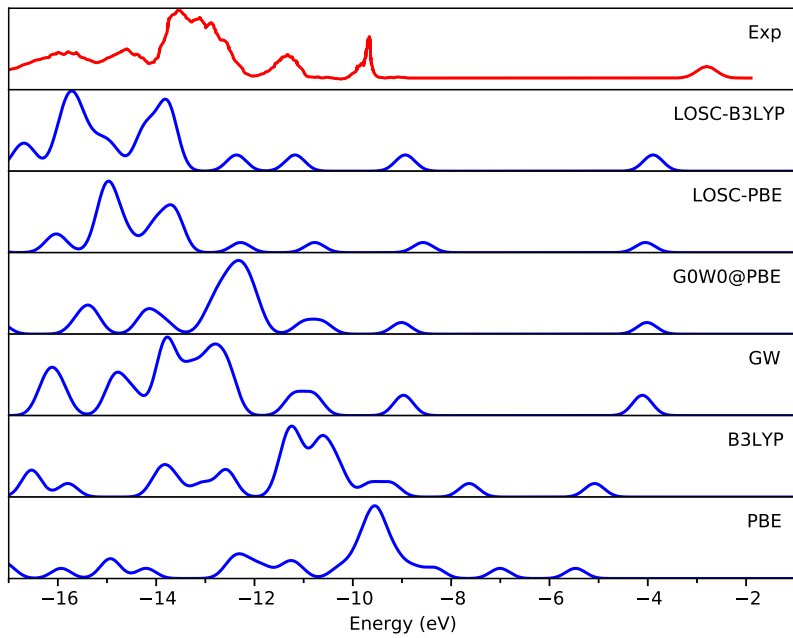


Figure S31: Photoemission spectrum of TCNQ. Experimental spectrum was obtained from Ref S23

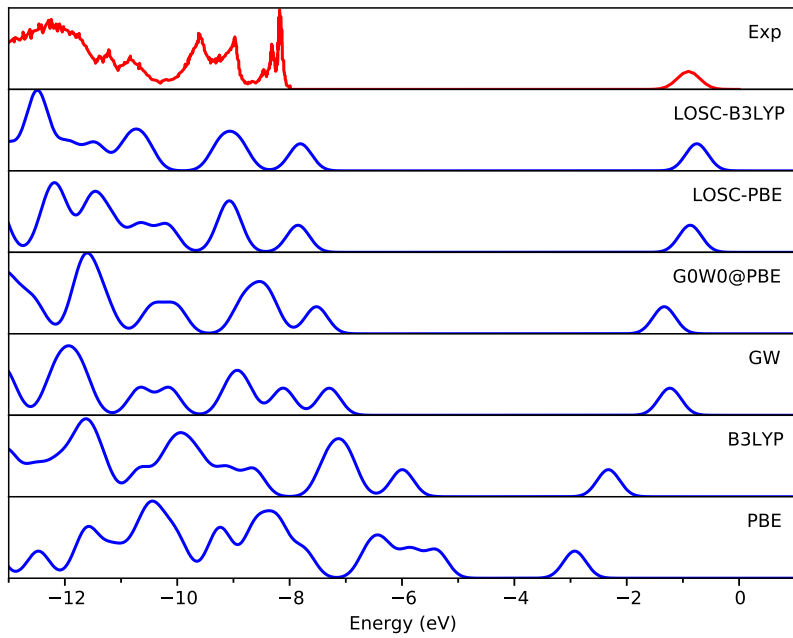


Figure S32: Photoemission spectrum of acridine. Experimental spectrum was obtained from Ref S21

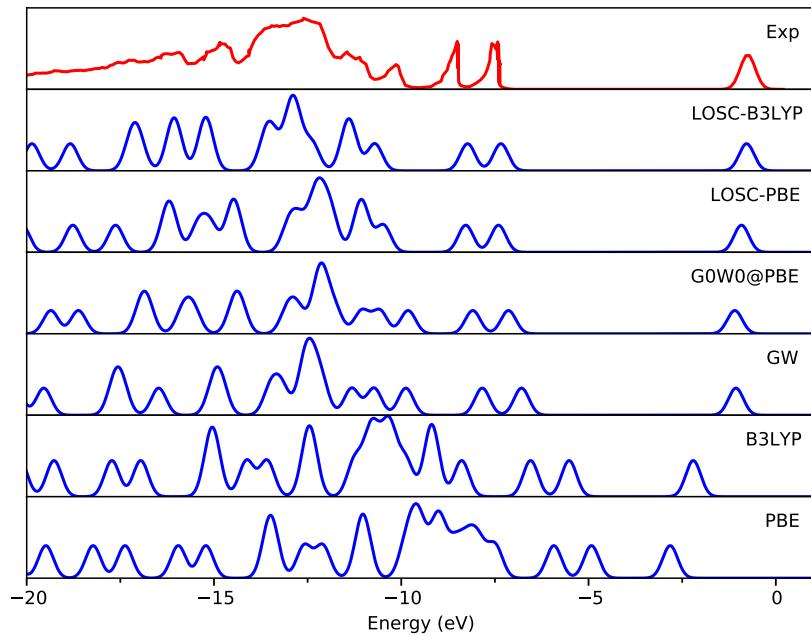


Figure S33: Photoemission spectrum of azulene. Experimental spectrum was obtained from Ref S28

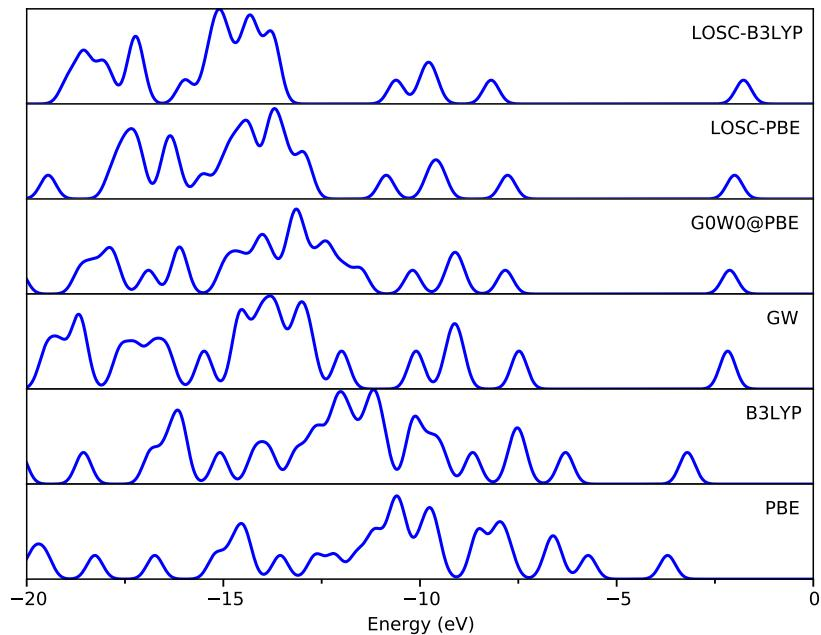


Figure S34: Photoemission spectrum of bodipy.

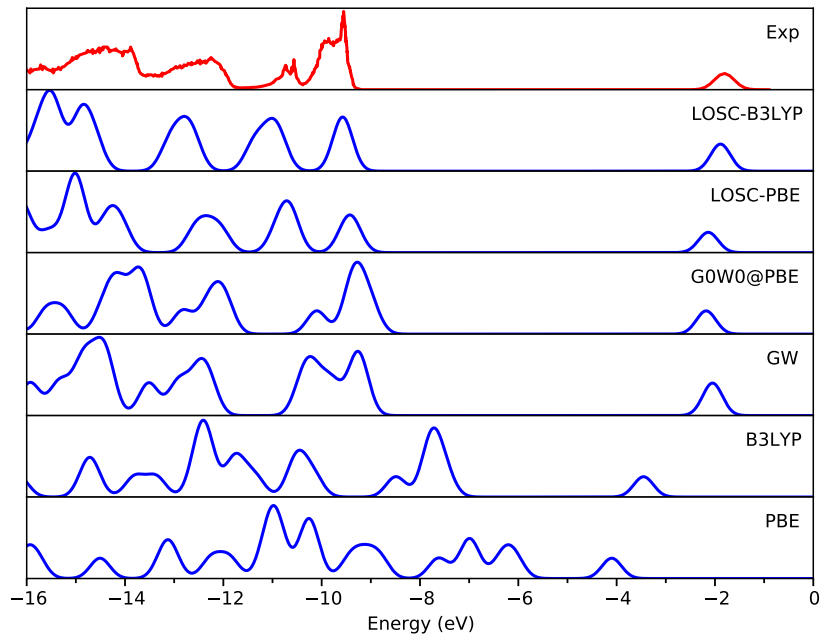


Figure S35: Photoemission spectrum of naphthalenedione. Experimental spectrum was obtained from Ref S29

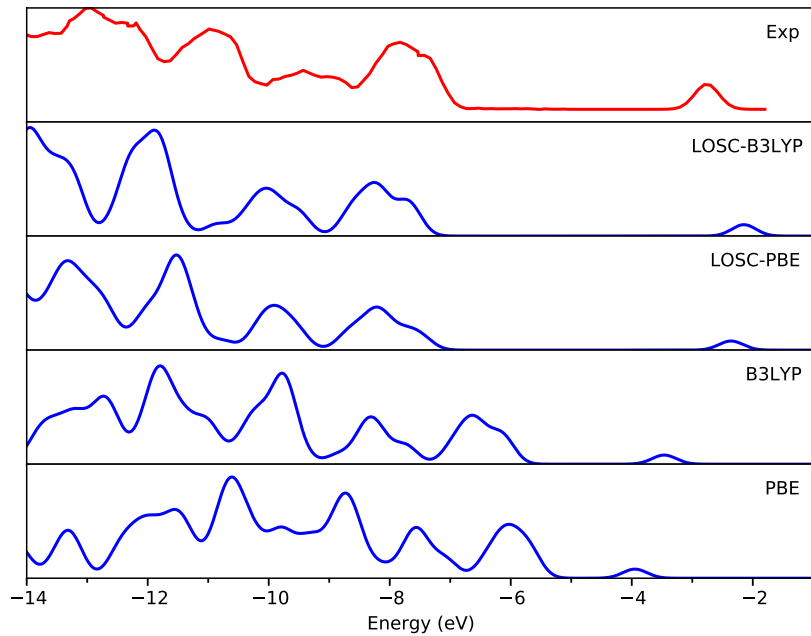


Figure S36: Photoemission spectrum of C_{70} . Experimental spectrum was obtained from Ref S30

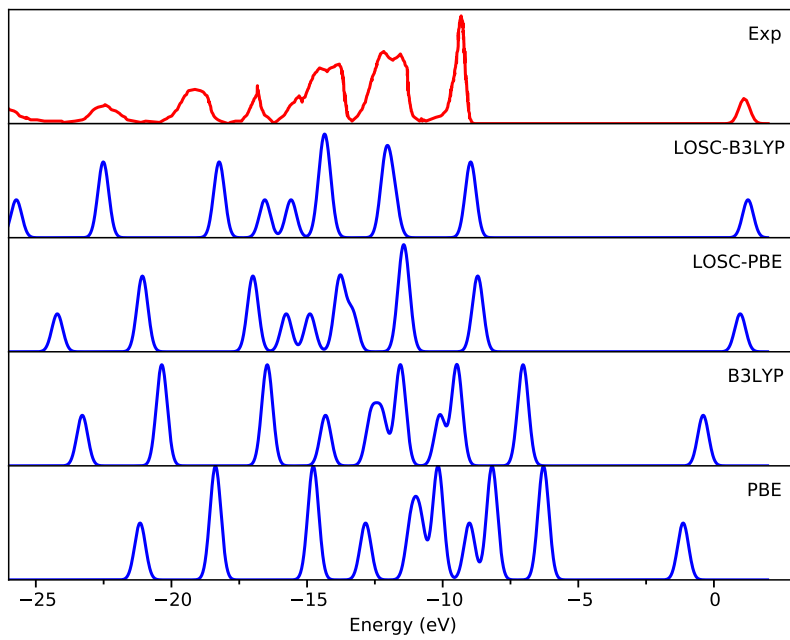


Figure S37: Photoemission spectrum of benzene. Experimental spectrum was obtained from Ref S31

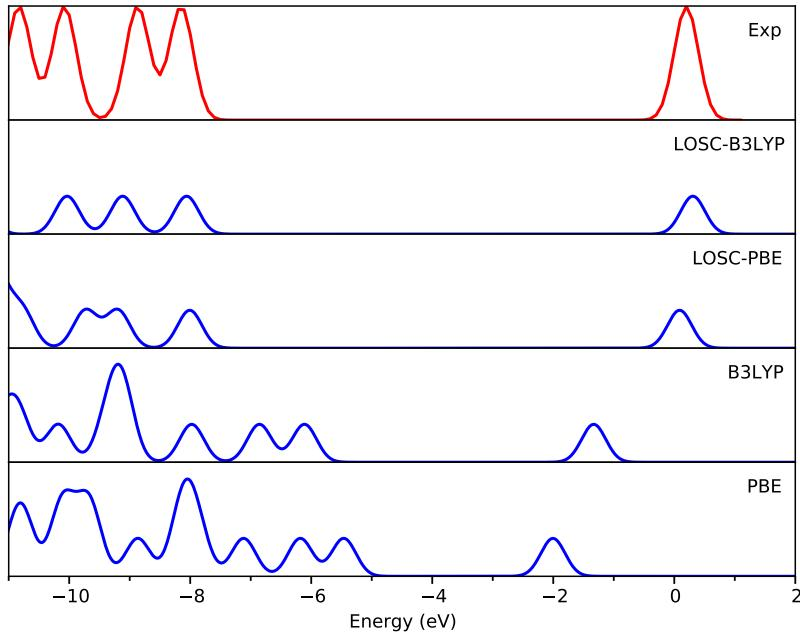


Figure S38: Photoemission spectrum of naphthalene. Experimental quasi-particle energies were obtained from Ref S6 and used to broaden the spectrum by Gaussian expansion with 0.2 eV.

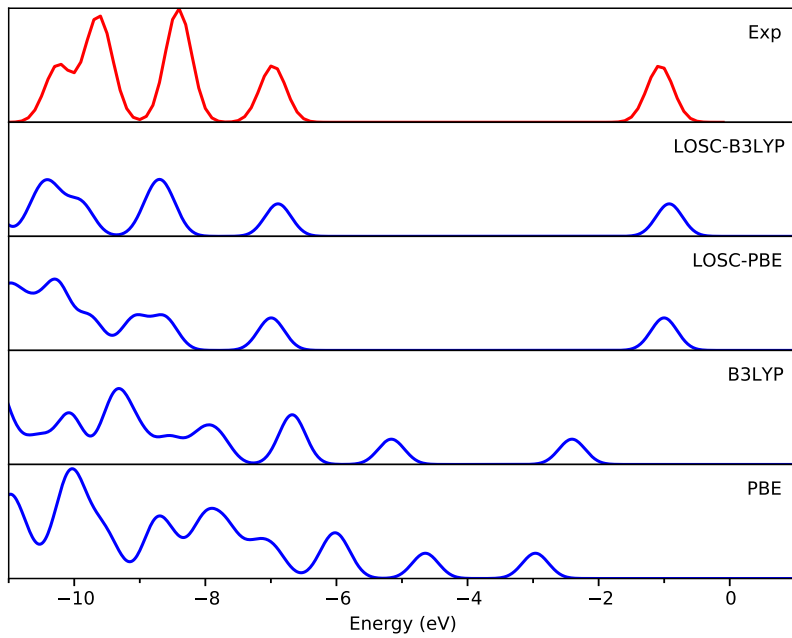


Figure S39: Photoemission spectrum of tetracene. Experimental quasi-particle energies were obtained from Ref S6 and used to broaden the spectrum by Gaussian expansion with 0.2 eV.

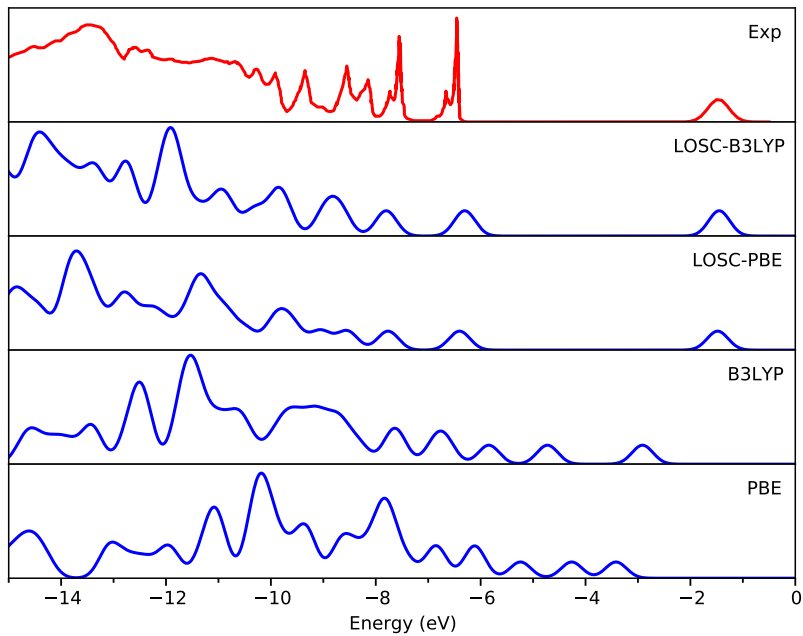


Figure S40: Photoemission spectrum of hexacene. Experimental spectrum was obtained from Ref S32

Quasi-particle energy

Table S1 and S2 show the detailed HOMO and LUMO energies for 40 molecules from density functional approximations (DFAs), L OSC-DFAs, self-consistent GW (sc GW), G_0W_0 @PBE and Δ SCF methods. Most of the test molecules are selected from Blase's^{S4} and Marom's^{S5} test set, if not specified. Geometries of Blase's test set are provided by Blase,^{S4} and geometries of Marom's test set can be found in Ref S5.

Table S3 shows the valence orbital energies from DFAs, L OSC-DFAs and Δ SCF methods. Test molecules includes polyacene ($n = 1 - 6$) and other three small molecules. Geometries of polyacene ($n = 1 - 6$) were optimized from B3LYP/6-31g* with Gaussian 09 pacage,^{S33} and attached at the end of SI. Other three geometries are obtained from Ref S34. The basis set used for DFT calculation is cc-pVTZ, if not specified. The fitting basis for L OSC is aug-cc-pVTZ.

Table S1: Comparison of (negative) HOMO energies (in eV) obtained from DFAs, LOSC-DFAs, self-consistent GW (sc GW), G_0W_0 @PBE, and Δ SCF (PBE and LOSC-PBE) methods with the experimental ionization potential.

Molecule	Exp ^f	sc GW ^f	G_0W_0 ^f	Δ PBE	Δ LOSC-PBE	LDA	PBE	B3LYP	LOSC-LDA	LOSC-PBE	LOSC-B3LYP
Anthracene ^d	7.40 ^e	6.77	7.04	7.09	7.47	5.16	4.94	5.51	7.62	7.40	7.30
Benzothiadiazole	9.00	NA	NA	8.73	8.86	6.36	6.13	6.85	8.77	8.54	8.75
Benzothiazole	8.80	NA	NA	8.50	8.80	6.17	5.96	6.69	8.84	8.63	8.63
C ₆₀ ^a	7.60	NA	NA	NA	NA	5.92	5.66	6.18	7.98	7.76	7.86
Fluorene	7.90	NA	NA	7.64	8.08	5.62	5.41	6.04	8.33	8.10	7.93
H ₂ P	6.90	NA	NA	6.75	6.78	5.22	4.98	5.48	7.37	7.23	7.05
H ₂ PC ^a	6.40	NA	NA	6.27	6.11	5.07	4.84	5.11	6.32	6.10	6.13
H ₂ TPP ^a	6.40	NA	NA	6.16	6.55	4.84	4.63	5.12	6.64	6.43	6.60
Pentacene ^d	6.60	NA	NA	6.16	6.69	4.63	4.41	4.87	6.75	6.52	6.42
PTCDA	8.20	NA	NA	7.86	8.59	6.40	6.13	6.68	8.94	8.63	8.41
Thiadiazole	10.10	NA	NA	10.13	10.13	7.10	6.90	7.73	9.63	9.44	9.75
thiophene	8.85	NA	NA	8.82	8.77	5.98	5.78	6.58	8.46	8.27	8.56
Benzoquinone	10.03	10.22	9.41	9.21	10.75	6.43	6.25	7.67	11.00	10.80	11.01
Cl ₄ -isobenzofuranedione	10.80	9.43	9.36	9.36	10.38	7.27	7.04	7.94	10.12	9.88	10.04
Dichlone	9.59	9.26	9.22	8.94	10.22	6.73	6.52	7.64	9.57	9.33	9.55
F ₄ -benzoquinone	10.83	10.65	10.27	10.03	10.86	7.52	7.23	8.39	10.08	9.80	10.48
Maleic anhydride	11.09	11.26	10.46	10.36	11.82	7.25	7.02	8.45	11.85	11.61	11.94
Nitrobenzene	9.93	9.54	9.68	9.65	10.73	6.95	6.70	7.87	9.77	9.67	9.81
Phenazine	8.38	7.74	7.92	7.90	8.39	5.84	5.66	6.39	8.41	8.10	8.25
Phthalimide	9.84	9.45	9.37	9.24	10.76	6.48	6.25	7.66	9.68	9.51	9.69
TCNE	11.78	11.36	11.19	11.15	12.50	8.83	8.55	9.42	12.54	12.30	12.30
Benzonitrile	9.75	9.29	9.34	9.53	10.11	7.04	6.81	7.58	9.80	9.58	9.71
Cl ₄ -benzoquinone	9.82	9.62	9.49	9.23	9.70	7.13	6.93	7.86	9.58	9.38	9.77
Dinitrobenzonitrile	N/A	10.55	10.52	11.21	11.76	7.89	7.61	8.90	11.52	11.21	11.26
F ₄ -benzenedicarbonitrile	10.65	10.21	9.92	10.14	10.31	7.63	7.35	8.39	9.58	9.31	10.01
Fumaronitrile	11.23	10.88	10.73	10.80	11.06	8.05	7.80	8.68	10.94	10.71	10.83
mDCBN	10.40	9.80	9.80	9.86	10.46	7.60	7.35	8.14	10.38	10.13	10.24
NDCA	8.98	8.45	8.62	8.69	9.56	6.67	6.42	7.10	9.43	9.18	9.19
Nitrobenzonitrile	10.40	10.02	10.02	9.94	11.60	7.45	7.19	8.37	10.51	10.28	10.53
Phthalic anhydride	10.18	9.90	9.96	9.79	11.00	7.05	6.81	8.23	10.19	9.97	10.15
TCNQ	9.61	8.97	9.01	9.04	8.91	7.27	7.01	7.63	8.87	8.57	8.93

Table S1. (Continued.)

Molecule	Exp ^f	scGW ^f	$G_0W_0^f$	ΔPBE	$\Delta\text{LOSC-PBE}$	LDA	PBE PBE	B3LYP B3LYP	LOSC- LDA	LOSC- PBE	LOSC- B3LYP
Acridine	7.99	7.30	7.52	7.52	8.06	5.62	5.38	5.99	8.05	7.85	7.81
Azulene	7.43	6.79	7.14	7.37	7.46	5.15	4.92	5.52	7.63	7.40	7.34
Bodipy	N/A	7.48	7.83	8.04	7.76	5.97	5.72	6.30	8.01	7.77	8.19
Naphthalenedione	9.54	9.21	8.99	8.75	10.39	6.29	6.08	7.48	9.58	9.35	9.57
C ₇₀ ^b	7.32 ^c	N/A	N/A	NA	NA	5.91	5.69	6.13	7.87	7.65	7.63
Benzene ^d	9.24 ^e	N/A	N/A	9.25	9.25	6.50	6.28	7.04	8.94	8.71	8.98
Naphthalene ^d	8.11 ^e	N/A	N/A	7.90	8.12	5.68	5.46	6.11	8.16	8.01	8.06
Tetracene ^d	6.97 ^e	N/A	N/A	6.55	7.03	4.87	4.64	5.16	7.20	7.00	6.89
Hexacene ^d	6.36 ^e	N/A	N/A	5.87	6.23	4.50	4.26	4.73	6.62	6.40	6.30
MAE		0.47	0.51	0.43	0.34	2.58	2.81	2.00	0.34	0.37	0.26
MSE		-0.43	-0.51	-0.42	0.20	-2.58	-2.81	-2.00	0.04	-0.18	-0.05

^a cc-pVDZ basis set used for DFT calculation.

S25

^b 6-31G basis set was used for DFT calculation. Molecular geometry was obtained from Ref S35.^c Ionization energy was read out from the experimental spectrum shown in Ref S30.^d Geometry was optimized from B3LYP/6-31G* with Gaussian 09 package.^{S33}^e Ref S1^f Ref S4 and S5, if not specified.

Table S2: Comparison of (negative) LUMO energies (in eV) obtained from DFAs, LOSC-DFAs, self-consistent GW (sc GW), G_0W_0 @PBE, and Δ SCF (PBE and LOSC-PBE) methods with the experimental electron affinity.

Molecule	Exp ^f	sc GW ^f	G_0W_0 ^f	Δ PBE	Δ LOSC- PBE	LDA	PBE PBE	B3LYP B3LYP	LOSC- LDA	LOSC- PBE	LOSC- B3LYP
Anthracene ^d	0.60 ^e	N/A	N/A	0.50	0.29	2.92	2.68	2.09	0.87	0.62	0.48
Benzothiadiazole	N/A	0.86	0.98	0.72	0.65	3.48	3.25	2.70	1.31	1.08	1.03
Benzothiazole	N/A	N/A	N/A	-0.37	-0.54	2.32	2.09	1.41	-0.12	-0.37	-0.49
C ₆₀ ^a	2.70	N/A	N/A	NA	NA	4.34	4.07	3.56	2.61	2.30	2.14
Fluorene	N/A	N/A	N/A	-0.30	-0.45	2.07	1.83	1.19	0.02	-0.29	-0.43
H ₂ P	N/A	N/A	N/A	1.31	1.74	3.29	3.04	2.60	1.89	1.71	1.37
H ₂ PC ^a	N/A	N/A	N/A	1.92	1.83	3.65	3.41	2.97	2.16	1.92	1.65
H ₂ TPP ^a	1.72	N/A	N/A	1.33	1.17	3.03	2.82	2.37	1.58	1.32	1.16
Pentacene ^d	N/A	N/A	N/A	1.50	1.24	3.55	3.31	2.80	1.59	1.38	1.47
PTCDA	N/A	N/A	N/A	2.90	2.63	4.90	4.60	4.18	3.02	2.69	2.71
Thiadiazole	N/A	N/A	N/A	-0.46	-0.47	2.88	2.66	1.99	0.59	0.37	0.18
thiophene	N/A	N/A	N/A	-1.48	-1.48	1.57	1.36	0.68	-0.55	-0.76	-0.99
Benzoquinone	1.88	2.13	2.27	1.68	1.67	4.76	4.48	3.81	2.93	2.65	2.35
Cl ₄ -isobenzofuranedione	1.96	2.32	2.25	1.70	1.54	4.28	3.99	3.43	2.14	1.87	1.74
Dichlone	2.21	2.55	2.58	2.00	1.94	4.59	4.32	3.73	2.68	2.41	2.23
F ₄ benzoquinone	2.69	3.07	2.91	2.17	2.17	5.31	4.98	4.49	3.52	3.19	3.04
Maleic anhydride	1.42	1.54	1.65	1.05	1.05	4.41	4.11	3.42	2.24	1.94	1.68
Nitrobenzene	1.01	1.18	1.24	0.55	0.28	3.65	3.35	2.71	0.64	0.35	0.34
Phenazine	1.31	1.70	1.77	1.16	1.11	3.60	3.34	2.75	1.54	1.29	1.20
Phthalimide	1.02	1.17	1.26	0.69	0.58	3.49	3.20	2.56	1.50	1.22	1.04
TCNE	3.17	3.80	3.78	3.13	3.22	6.03	5.74	5.22	4.08	3.78	3.70
Benzonitrile	0.26	0.26	0.40	-0.15	-0.15	2.71	2.45	1.77	0.58	0.28	0.28
Cl ₄ -benzoquinone	2.77	3.15	3.11	2.50	2.53	5.21	4.94	4.39	3.21	2.96	3.01
Dinitrobenzonitrile	2.16	2.53	2.46	2.12	1.36	4.79	4.47	3.88	1.86	1.54	1.60
F ₄ -benzenedicarbonitrile	1.89	2.38	2.18	1.59	1.46	4.36	4.05	3.57	2.39	2.09	2.11
Fumaronitrile	1.25	1.49	1.68	1.11	1.11	4.31	4.04	3.37	2.07	1.79	1.61
mDCBN	0.91	1.16	1.27	0.77	0.69	3.50	3.23	2.58	1.55	1.28	1.07
NDCA	N/A	1.85	1.91	1.40	1.10	3.87	3.59	3.01	1.90	1.62	1.43
Nitrobenzonitrile	1.71	2.02	2.01	1.49	1.14	4.33	4.03	3.44	1.54	1.21	1.27
Phthalic anhydride	1.26	1.44	1.52	0.96	0.87	3.81	3.52	2.87	1.75	1.46	1.36

Table S2. (Continued.)

Molecule	Exp ^f	scGW ^f	$G_0W_0^f$	ΔPBE	$\Delta\text{LOSC-PBE}$	LDA	PBE PBE	B3LYP B3LYP	LOSC- LDA	LOSC- PBE	LOSC- B3LYP
TCNQ	2.80	4.11	4.02	3.41	3.77	5.75	5.47	5.08	4.31	4.05	3.89
Acridine	0.90	1.23	1.33	0.80	0.72	3.18	2.93	2.33	1.13	0.87	0.75
Azulene	0.75	1.07	1.10	0.43	0.60	3.07	2.82	2.20	1.17	0.92	0.78
Bodipy	N/A	2.18	2.13	1.43	1.87	3.96	3.70	3.20	2.25	2.00	1.77
Naphthalenedione	1.81	2.05	2.18	1.62	1.56	4.38	4.10	3.45	2.43	2.14	1.89
C ₇₀ ^b	2.76 ^c	N/A	N/A	2.45	2.31	4.18	3.95	3.46	2.54	2.36	2.15
Benzene ^d	-1.12 ^e	N/A	N/A	-1.63	-1.64	1.38	1.13	0.39	-0.73	-0.97	-1.26
Naphthalene ^d	-0.20 ^e	N/A	N/A	-0.36	-0.40	2.25	2.00	1.33	0.16	-0.09	-0.31
Tetracene ^d	1.06 ^e	N/A	N/A	1.08	0.85	3.22	2.96	2.41	1.26	1.00	0.92
Hexacene ^d	1.47 ^e	N/A	N/A	1.82	1.88	3.67	3.42	2.91	1.76	1.48	1.45
MAE	0.34	0.37	0.26	0.38	2.43	2.16	1.57	0.48	0.33	0.29	
MSE	0.34	0.37	-0.19	-0.28	2.43	2.16	1.57	0.39	0.11	-0.02	

S27

^a cc-pVDZ basise set was used for DFT calculation.^b 6-31G basise set was used for DFT calculation. Molecular geometry was obtained form Ref S35.^c Ref S36^d Geometry was optimized from B3LYP/6-31G* with Gaussian 09 package.^{S33}^e Ref S1^f Ref S4 and S5, if not specified.

Table S3: Occupied orbital energies (in eV) obtained from DFAs, LOSC-DFAs and Δ SCF methods (B3LYP and LOSC-B3LYP) compared with the experimental reference.

Molecule	State	Exp ^a	Δ B3LYP	Δ LOSC-B3LYP	LDA	PBE	BLYP	B3LYP	LOSC-LDA	LOSC-PBE	LOSC-BLYP	LOSC-B3LYP
Benzene	E_{1g}	9.24	9.07	9.06	6.50	6.28	6.09	7.04	8.94	8.71	8.51	8.98
	E_{1g}	9.24	9.08	9.07	6.50	6.28	6.09	7.04	8.93	8.70	8.50	8.96
	A_{2u}	12.25	NA	NA	8.26	8.18	8.12	9.48	11.41	11.33	11.54	12.12
	MAE		0.17	0.18	3.16	3.33	3.48	2.39	0.48	0.66	0.73	0.22
Naphthalene	A_u	8.15	7.71	8.00	5.68	5.46	5.26	6.11	8.16	8.01	7.71	8.06
	B_{1u}	8.87	8.47	9.03	6.40	6.18	5.97	6.86	9.37	9.20	8.84	9.12
	B_{2g}	10.08	9.44	9.73	7.34	7.12	6.91	7.98	9.84	9.73	9.37	10.03
	B_{3g}	10.83	10.32	11.15	7.98	7.87	7.81	9.13	11.25	11.17	11.12	11.54
	MAE		0.50	0.25	2.63	2.82	3.00	1.97	0.29	0.29	0.37	0.27
Anthracene S28	B_{2g}	7.41	6.89	7.30	5.19	4.97	4.76	5.54	7.66	7.44	7.23	7.36
	B_{3g}	8.54	8.10	8.90	6.36	6.13	5.92	6.76	9.28	9.11	8.87	9.01
	A_u	9.19	8.38	9.24	6.68	6.45	6.24	7.22	9.52	9.36	9.15	9.43
	B_{2g}	10.18	NA	NA	7.68	7.45	7.24	8.35	10.36	10.20	9.99	10.52
	B_{1u}	10.28	9.52	10.52	7.83	7.60	7.38	8.50	10.84	10.67	10.44	10.86
	MAE		0.63	0.19	2.37	2.60	2.81	1.84	0.41	0.24	0.18	0.33
Teracene	A_u	6.97	6.35	6.86	4.87	4.64	4.44	5.16	7.20	7.00	6.86	6.89
	AB_{2g}	8.41	7.61	8.54	6.16	5.93	5.72	6.64	8.82	8.62	8.50	8.60
	B_{1u}	8.41	7.84	8.81	6.35	6.11	5.89	6.71	9.27	9.08	8.83	8.80
	A_u	9.56	8.66	9.70	7.19	6.95	6.74	7.80	9.93	9.76	9.61	9.90
	B_{3g}	9.70	8.92	10.08	7.48	7.25	7.02	8.08	10.50	10.30	10.06	10.32
	B_{2g}	10.25	9.46	9.93	7.85	7.62	7.40	8.54	10.41	10.22	10.04	10.54
	MAE		0.74	0.25	2.23	2.47	2.68	1.73	0.47	0.29	0.21	0.32
Pentacene	B_{2g}	6.61	5.96	6.47	4.66	4.42	4.22	4.90	6.78	6.59	6.42	6.46
	A_u	7.92	7.04	7.88	5.77	5.54	5.33	6.19	8.26	8.00	7.83	8.16
	B_{3g}	8.32	7.64	8.79	6.34	6.10	5.87	6.68	9.24	9.04	8.80	8.97
	B_{2g}	9.01	8.02	9.20	6.74	6.51	6.29	7.29	9.49	9.28	9.15	9.16
	B_{1u}	9.39	8.50	9.79	7.24	7.00	6.78	7.78	10.21	9.98	9.77	10.14
	A_u	9.80	8.79	10.04	7.48	7.24	7.02	8.12	10.11	9.85	9.70	10.11
	B_{2g}	10.23	NA	NA	7.88	7.72	7.50	8.65	11.48	10.46	10.28	10.67

Table S3. (Continued.)

Molecule	State	Exp ^a	Δ B3LYP	Δ LOSC-B3LYP	LDA	PBE	BLYP	B3LYP	LOSC-LDA	LOSC-PBE	LOSC-BLYP	LOSC-B3LYP
	<i>MAE</i>	0.85	0.25	2.17	2.39	2.61	1.67	0.61	0.28	0.20	0.38	
Hexacene	<i>A_u</i>	6.36	5.67	5.97	4.50	4.26	4.06	4.73	6.62	6.40	6.18	6.30
	<i>B_{2g}</i>	7.35	6.60	7.41	5.48	5.24	5.03	5.84	7.95	7.77	7.56	7.80
	<i>B_{3u}</i>	8.12	7.49	8.36	6.33	6.09	5.86	6.66	9.26	9.06	8.78	8.96
	<i>A_u</i>	8.56	7.50	8.29	6.37	6.14	5.92	6.87	9.09	8.54	8.35	8.68
	<i>B_{1g}</i>	9.36	8.18	9.38	7.07	6.83	6.60	7.57	10.01	9.79	9.55	9.91
	<i>B_{2g}</i>	9.36	8.24	8.83	7.11	6.87	6.65	7.70	9.69	9.56	9.35	9.76
	<i>A_u</i>	9.95	8.83	9.43	7.66	7.43	7.20	8.32	10.42	9.97	9.82	10.32
	<i>B_{3u}</i>	9.95	9.14	10.62	7.88	7.75	7.55	8.66	11.51	11.36	10.57	11.02
	<i>MAE</i>	0.92	0.34	2.08	2.30	2.52	1.58	0.69	0.43	0.28	0.48	
Thiophene	<i>1A₂</i>	8.87	8.65	8.56	5.98	5.78	5.59	6.58	8.46	8.27	8.08	8.56
	<i>3B₁</i>	9.52	9.09	9.02	6.38	6.21	6.02	7.02	8.85	8.69	8.50	8.99
	<i>11A₁</i>	12.10	11.46	11.52	8.49	8.37	8.22	9.46	11.58	11.45	11.34	11.96
	<i>2B₁</i>	12.70	12.19	12.19	9.45	9.26	9.03	10.39	12.05	11.87	11.63	12.46
	<i>7B₂</i>	13.30	12.36	12.30	9.47	9.38	9.24	10.55	12.10	12.02	11.93	12.65
	<i>10A₁</i>	13.90	12.59	12.69	9.60	9.48	9.37	10.78	12.28	12.14	12.09	13.10
	<i>6B₂</i>	14.30	12.96	13.01	9.95	9.87	9.78	11.20	12.59	12.57	12.50	13.29
	<i>9A₁</i>	16.60	15.45	15.46	12.61	12.50	12.32	13.92	15.18	15.08	14.93	15.94
	<i>5B₂</i>	17.60	16.46	16.24	13.50	13.47	13.29	14.99	15.93	15.90	15.78	17.00
	<i>8A₁</i>	18.30	16.80	16.81	13.76	13.73	13.56	15.30	16.19	16.18	16.09	17.32
	<i>MAE</i>	0.92	0.94	3.80	3.92	4.08	2.70	1.20	1.30	1.43	0.59	
Ethylene	<i>1B_{3u}</i>	10.68	10.53	10.53	6.92	6.73	6.55	7.62	10.63	10.45	10.26	10.59
	<i>1B_{3g}</i>	12.80	12.39	12.39	8.48	8.51	8.47	9.82	11.33	11.35	11.31	12.10
	<i>3A_g</i>	14.80	14.24	14.24	10.23	10.14	10.08	11.56	13.92	13.83	13.78	14.52
	<i>1B_{2u}</i>	16.00	15.45	15.45	11.56	11.49	11.39	12.93	14.80	14.72	14.61	15.50
	<i>2B_{1u}</i>	19.10	18.20	18.20	14.16	14.22	14.08	15.89	17.34	17.41	17.27	18.44
	<i>2A_g</i>	23.60	23.25	23.25	18.72	18.79	18.60	20.82	23.18	23.25	23.06	24.40
	<i>MAE</i>	0.49	0.49	4.49	4.52	4.63	3.06	0.96	0.99	1.12	0.51	
Water	<i>1B₁</i>	12.62	12.60	12.60	6.99	6.83	6.77	8.49	13.11	12.98	12.92	13.42
	<i>3A₁</i>	14.74	14.71	14.71	9.02	8.94	8.85	10.55	15.13	15.03	14.94	15.41
	<i>1B₂</i>	18.55	18.74	18.74	12.98	12.90	12.81	14.44	18.46	18.38	18.28	18.83

Table S3. (Continued.)

Molecule	State	Exp ^a	Δ B3LYP	Δ LOSC-B3LYP	LDA	PBE	BLYP	B3LYP	LOSC-LDA	LOSC-PBE	LOSC-BLYP	LOSC-B3LYP
	MAE	0.08	0.08	5.64	5.75	5.83	4.14	0.32	0.27	0.26	0.58	
MAE Polyacene		0.73	0.26	2.33	2.55	2.76	1.79	0.53	0.35	0.29	0.36	
MSE Polyacene		-0.73	0.04	-2.33	-2.55	-2.76	-1.79	0.42	0.19	-0.02	0.29	
Total MAE		0.70	0.41	3.06	3.23	3.40	2.24	0.69	0.60	0.60	0.43	
Total MSE		-0.69	-0.22	-3.06	-3.23	-3.40	-2.24	-0.06	-0.23	-0.41	0.08	

^a The experimental data for polyacence ($n = 1 - 6$) were obtained from Ref S6, other experimental data were obtained from Ref S37.

Excitation energy

Table S4 - S6 show the detailed low-lying excitation energies of 16 molecular test set from different methods. The basis set used for DFT calculation was 6-311++G(3df, 3pd), if not specified. Gaussian 09 package^{S33} was applied to perform TD-DFT calculation, and cc-pVTZ were used as basis set. Geometries were obtained from Ref S38. Table S7 - S12 show detailed excitation energies of 4 atoms (Li, Be, Mg and Na) in which Rydberg excited states were concerned. To describe Rydberg states of these 4 atoms, greatly diffused basis set were used to perform the calculation. Here even-tempered basis set was built, with its Gaussian orbital exponents α satisfying $\alpha_i = 2^{i-1}\alpha_1$. Each of the even-tempered basis contains 17s, 15p and 11d functions with the smallest exponents being $\alpha_1 = 0.000976525, 0.000976525$, and 0.0039062500 , respectively. For excitation calculation from DFT by orbital energies, unrestricted calculation were applied for all test cases.

Table S4: Low-lying vertical excitation energies (in eV) obtained from N-1 system with Hartree Fock (HF), DFAs, LOSC-DFAs, TD-B3LYP and Δ SCF-B3LYP.

Molecule	MO	Ref ^a	TD-B3LYP	Δ SCF-B3LYP	BLYP	B3LYP	LDA	HF	LOSC-BLYP	LOSC-B3LYP	LOSC-LDA
Ethene	$^3B_{1u}$	4.50	4.05	4.38	4.61	4.43	4.90	3.09	4.15	4.05	4.40
Ethene	$^1B_{1u}$	7.80	7.38	7.09	7.46	7.75	7.27	6.61	6.61	7.00	6.52
Furan	3B_2	4.17	3.70	3.98	4.05	3.95	4.31	2.95	3.74	3.71	3.88
Furan	3A_2	5.99*	5.48	5.75	5.78	5.84	5.99	3.99	5.63	5.71	5.71
Furan	1B_2	6.32	5.94	5.78	5.73	6.11	5.60	5.07	5.76	6.08	5.43
Furan	1A_2	6.03*	5.51	5.88	6.91	7.27	6.91	4.92	6.86	7.15	6.69
Benzoquinone	$^3B_{1g}$	2.51	1.93	2.08	1.68	2.08	1.60	3.28	2.08	2.36	1.99
Benzoquinone	$^3B_{3u}$	5.38*	5.18	5.12	4.76	5.40	4.66	7.21	5.36	5.81	5.28
Benzoquinone	$^1B_{1g}$	2.78	2.43	2.38	1.95	2.41	1.94	4.11	2.30	2.64	2.30
Benzoquinone	$^1B_{3u}$	5.60	5.38	5.51	4.85	5.49	4.78	7.14	5.45	5.89	5.40
cyclopentadiene	3B_2	3.25	2.74	3.11	3.21	3.12	3.46	2.30	2.82	2.82	3.06
cyclopentadiene	3A_2	5.61*	5.09	5.37	5.65	5.76	5.85	3.60	5.49	5.59	5.67
cyclopentadiene	1B_2	5.55	4.95	4.82	4.74	5.06	4.66	4.93	4.29	4.70	4.22
cyclopentadiene	1A_2	5.65*	5.11	5.40	6.79	7.14	6.77	4.66	6.38	6.75	6.44
butadiene	3B_u	3.20	2.79	3.20	3.22	3.19	3.40	2.54	2.76	3.06	2.90
butadiene	3B_g	6.22*	5.67	5.80	5.86	6.02	6.05	4.09	5.53	5.96	5.68
butadiene	1B_u	6.18	5.56	5.13	4.86	5.39	4.72	5.67	5.08	5.74	4.80
butadiene	1B_g	6.26*	5.70	6.10	6.80	7.04	6.86	4.73	6.81	7.27	6.78
hexatriene	3B_u	2.40	2.12	2.52	2.49	2.51	2.62	1.92	2.76	2.53	2.94
hexatriene	3A_u	5.68*	5.22	4.99	4.82	5.10	4.95	3.55	5.54	5.44	5.72
hexatriene	1B_u	5.10	4.60	4.11	3.66	4.22	3.54	5.20	4.02	4.70	3.97
hexatriene	1A_u	5.71*	5.24	5.79	5.58	6.05	5.60	3.98	6.09	6.36	6.26
octetraene	3B_u	2.20	1.71	2.10	2.05	2.11	2.16	1.57	2.76	2.33	2.91
octetraene	1B_u	4.66	3.96	3.47	2.96	3.52	2.86	4.86	3.93	3.92	3.88
cyclopropene	3B_2	4.34	3.70	4.03	4.22	4.19	4.38	3.16	4.49	4.34	4.69
cyclopropene	1B_2	7.06	6.09	6.27	6.29	6.69	5.97	6.20	6.23	6.50	6.07
norbornadiene	3A_2	3.72	3.10	3.54	3.62	3.71	3.73	3.50	4.00	3.92	4.08
norbornadiene	1A_2	5.34	4.70	4.73	4.64	4.90	4.56	4.89	4.82	4.87	4.77
s-tetrazine	3B_u	1.89	1.47	1.62	1.32	1.63	1.21	2.48	1.28	1.72	1.22

Table S4. (Continued.)

Molecule	MO	Ref ^a	TD-B3LYP	Δ SCF-B3LYP	BLYP	B3LYP	LDA	HF	LOSC-BLYP	LOSC-B3LYP	LOSC-LDA
s-tetrazine	3A_u	3.52	3.15	3.34	2.98	3.45	2.85	4.90	2.95	3.54	2.86
s-tetrazine	1B_u	2.24	2.27	2.12	1.77	2.17	1.74	3.57	1.73	2.25	1.74
s-tetrazine	1A_u	3.48	3.54	N/A	3.13	3.59	3.06	4.88	3.08	3.66	3.06
formaldehyde	3A_2	3.50	3.10	3.19	3.37	3.17	3.38	1.17	2.94	2.73	3.08
formaldehyde	1A_2	3.88	3.83	3.48	3.63	3.41	3.89	1.20	3.09	2.87	3.47
acetone	3B_1	4.05	3.68	3.75	3.95	3.78	4.09	1.82	3.36	3.24	3.53
acetone	3B_2	5.87*	5.71	6.20	7.95	7.47	8.38	2.81	6.23	5.99	6.78
acetone	1B_1	4.40	4.30	4.00	4.19	4.01	4.50	1.89	3.57	3.43	3.90
acetone	1B_2	5.92*	5.77	6.24	8.02	7.54	8.46	2.85	6.30	6.01	6.65
pyridine	3B_1	4.25	4.05	4.42	4.37	4.42	4.43	2.82	3.22	4.21	2.93
pyridine	3A_2	5.28	4.96	N/A	4.99	4.60	5.15	3.54	3.84	4.40	3.65
pyridine	1B_1	4.59	4.76	4.45	4.80	5.54	4.89	2.09	3.57	5.29	3.33
pyridine	1A_2	5.11	5.10	N/A	5.36	6.40	5.32	3.58	4.13	6.07	3.77
pyridazine	1B_1	3.78	3.60	3.51	3.61	3.64	3.64	3.86	2.41	2.69	2.40
pyridazine	1A_2	4.32	4.19	N/A	4.25	4.25	4.26	2.59	3.03	3.28	2.99
pyrizine	1B_u	3.95	3.93	3.81	3.53	3.90	3.52	5.12	3.57	3.55	3.55
pyrizine	1A_u	4.81	4.69	N/A	4.39	4.76	4.34	5.56	4.35	4.35	4.30
pyrimidine	1B_1	4.55	4.25	4.11	3.97	4.17	4.01	3.40	3.72	3.77	3.75
pyrimidine	1A_2	4.91	4.60	N/A	4.37	4.59	4.40	3.95	4.19	4.23	4.19
MAE			0.38	0.35	0.53	0.42	0.58	1.35	0.63	0.49	0.67
MSE			-0.37	-0.31	-0.22	-0.01	-0.16	-0.83	-0.44	-0.19	-0.42

^a Reference data labeled with an asterisk are obtained from CC2/aug-cc-pVTZ calculation with TURBOMOLE package,^{S39} other reference values were obtained from Ref S40.

Table S5: Low-lying vertical excitation energies (in eV) obtained from N+1 system with Hartree Fock (HF), DFAs, LOSC-DFAs, TD-B3LYP and Δ SCF-B3LYP.

Molecule	MO	Ref ^a	TD-B3LYP	Δ SCF-B3LYP	BLYP	B3LYP	LDA	HF	LOSC-BLYP	LOSC-B3LYP	LOSC-LDA
Ethene	$^1B_{1u}$	7.80	7.38	7.09	4.89	5.61	5.07	7.63	7.78	7.92	7.92
Ethene	$^3B_{1u}$	4.50	4.05	4.38	4.86	5.59	5.02	7.65	7.75	7.88	7.89
Furan	1B_2	6.32	5.94	5.78	3.96	4.67	4.15	6.90	6.15	6.37	6.38
Furan	3B_2	4.17	3.70	3.98	3.95	4.65	4.12	6.90	6.22	6.33	6.34
Benzoquinone	$^1B_{1g}$	2.78	2.43	2.38	1.81	2.39	1.79	4.71	4.67	4.55	4.51
Benzoquinone	$^3B_{1g}$	2.51	1.93	2.08	1.54	2.06	1.45	2.71	4.34	4.20	4.15
cyclopentadiene	1B_2	5.55	4.95	4.82	3.64	4.32	3.75	6.63	5.74	5.99	5.75
cyclopentadiene	3B_2	3.25	2.74	3.11	3.63	4.31	3.66	6.63	5.73	5.98	5.67
butadiene	1B_u	6.18	5.56	5.13	3.92	4.71	3.95	6.68	6.36	5.74	6.14
butadiene	3B_u	3.20	2.79	3.20	3.52	3.27	3.50	6.67	5.81	3.88	5.56
hexatriene	1B_u	5.10	4.60	4.11	3.25	3.88	3.22	6.20	4.13	4.71	4.28
hexatriene	3B_u	2.40	2.12	2.52	2.45	2.55	2.56	6.17	3.24	2.92	3.40
octetraene	1B_u	4.66	3.96	3.47	2.72	3.30	2.68	5.87	4.12	3.83	3.99
octetraene	3B_u	2.20	1.71	2.10	2.04	2.13	2.12	1.82	3.17	2.61	3.26
cyclopropene	1B_2	7.06	6.09	6.27	4.42	5.18	4.49	7.83	6.74	7.04	6.74
cyclopropene	3B_2	4.34	3.70	4.03	4.40	5.16	4.45	7.81	6.72	7.02	6.71
norbornadiene	1A_2	5.34	4.70	4.73	3.76	4.51	3.77	6.99	6.56	6.72	6.42
norbornadiene	3A_2	3.72	3.10	3.54	3.75	4.50	3.66	6.98	6.55	6.72	6.33
s-tetrazine	1B_u	2.24	2.27	2.12	1.74	2.09	1.74	3.11	2.96	2.86	3.00
s-tetrazine	3B_u	1.89	1.47	1.62	1.37	1.61	1.30	1.90	2.64	2.60	2.57
formaldehyde	1A_2	3.88	3.83	3.48	3.34	3.67	3.28	5.65	6.18	4.78	5.84
formaldehyde	3A_2	3.50	3.10	3.19	3.19	3.29	3.02	4.82	5.99	4.35	5.55
acetone	1B_1	4.40	4.30	4.00	3.97	5.08	N/A	8.79	7.51	7.77	N/A
acetone	3B_1	4.05	3.68	3.75	3.95	5.07	N/A	8.80	7.52	7.75	N/A
pyridine	1B_1	4.59	4.76	4.45	4.12	5.36	4.00	7.70	7.67	8.16	7.29
pyridine	3B_1	4.25	4.05	4.42	4.04	5.29	3.85	7.69	7.61	8.09	7.16
pyridazine	1B_1	3.78	3.60	3.51	2.93	3.40	2.83	6.27	4.96	4.40	4.64
pyrizine	1B_u	3.95	3.93	3.81	3.28	3.74	3.27	5.27	6.40	5.58	5.57

Table S5. (Continued.)

Molecule	MO	Ref ^a	TD-B3LYP	Δ SCF-B3LYP	BLYP	B3LYP	LDA	HF	LOSC-BLYP	LOSC-B3LYP	LOSC-LDA
pyrimidine	1B_1	4.55	4.25	4.11	3.64	4.07	3.58	7.81	6.82	5.75	6.57
MAE				0.41	0.40	0.91	0.78	0.98	2.05	1.72	1.51
MSE				-0.40	-0.38	-0.83	-0.23	-0.87	2.01	1.58	1.39

^a Reference values were obtained from Ref S40.

Table S6: Errors (in eV) of the vertical excitation energies from $(N + 1)$ -system with HF, DFAs, LOSC-DFAs, TD-B3LYP, and Δ SCF-DFT. T1 stands for triplet HOMO to LUMO excitation, and S1 stands for singlet HOMO to LUMO excitation.

Method	T1		S1		Total	
	MAE	MSE	MAE	MSE	MAE	MSE
HF	2.56	2.51	1.64	1.62	2.05	2.01
BLYP	0.28	-0.10	1.43	-1.43	0.91	-0.83
B3LYP	0.58	0.42	0.94	-0.76	0.78	-0.23
LDA	0.35	-0.10	1.48	-1.48	0.98	-0.87
LOSC-BLYP	2.25	2.25	1.29	1.04	1.72	1.58
LOSC-B3LYP	2.03	2.03	1.08	0.87	1.51	1.39
LOSC-LDA	2.05	2.05	1.00	0.75	1.47	1.33
TD-B3LYP	0.45	-0.45	0.38	-0.35	0.41	-0.40
Δ SCF-B3LYP	0.20	-0.16	0.56	-0.56	0.40	-0.38

Table S7: Doublet excitation energy (in eV) of atom Li. Experimental data were obtained from Ref S41

AO	Exp	LDA	BLYP	B3LYP	LOSC-LDA	LOSC-BLYP	LOSC-B3LYP
2p	1.85	1.95	2.07	2.06	1.96	2.18	2.08
3s	3.37	4.30	4.80	4.56	2.78	3.53	3.46
3p	3.83	4.72	5.33	5.07	3.15	4.02	3.90
3d	3.88	4.98	5.56	5.27	3.43	4.29	4.15
4s	4.34	5.40	6.23	5.84	3.31	4.30	4.24
4p	4.52	5.56	6.42	6.03	3.43	4.45	4.43
4d	4.54	5.66	6.52	6.12	3.58	4.55	4.53
5s	4.75	5.85	6.81	6.19	3.54	4.66	4.39
5p	4.84	5.92	6.92	6.49	3.60	4.78	4.72
5d	4.85	-	7.04	6.62	-	5.00	4.98
6s	4.96	6.07	7.11	6.62	3.61	4.74	4.69
6p	5.01	6.12	7.12	6.68	3.67	4.71	4.76
MAE		0.97	1.77	1.40	0.91	0.17	0.16
MSE		0.97	1.77	1.40	-0.89	0.04	-0.03

Table S8: Doublet excitation energy (in eV) of atom Na. Experimental data were obtained from Ref S41

AO	Exp	LDA	BLYP	B3LYP	LOSC-LDA	LOSC-BLYP	LOSC-B3LYP
3p	2.10	2.86	3.04	2.86	2.48	2.70	2.60
4s	3.19	4.52	5.34	4.83	3.29	4.04	3.82
3d	3.62	5.10	5.81	5.33	3.93	4.66	4.38
4p	3.75	5.15	5.89	5.39	3.81	4.49	4.28
5s	4.12	5.64	6.37	5.87	3.90	4.63	4.48
4d	4.28	5.85	6.53	6.04	4.14	4.93	4.73
5p	4.34	5.88	6.62	6.11	4.08	4.80	4.66
6s	4.51	6.10	6.82	6.32	4.15	4.89	4.77
6p	4.62	6.21	6.95	6.44	4.24	4.95	4.85
5d	4.59	6.34	7.00	6.52	4.60	5.29	5.16
7s	4.71	6.41	7.06	6.56	4.34	4.97	4.92
7p	4.78	6.78	7.13	6.63	4.35	5.08	4.99
MAE		1.52	2.16	1.69	0.25	0.57	0.42
MSE		1.52	2.16	1.69	-0.11	0.57	0.42

Table S9: Singlet excitation energy (in eV) of atom Be. Experimental data were obtained from Ref S41

AO	Exp	LDA	BLYP	B3LYP	LOSC-LDA	LOSC-BLYP	LOSC-B3LYP
2p	5.28	5.68	2.49	5.60	5.56	4.70	5.59
3s	6.78	9.02	6.14	8.98	7.27	7.54	7.42
3p	7.46	9.77	6.66	9.54	7.90	7.86	7.88
3d	7.99	10.29	7.30	10.08	8.44	8.32	8.34
4s	8.09	10.67	6.91	9.96	8.17	7.50	7.86
4p	8.31	10.90	7.11	10.19	8.37	7.79	8.14
4d	8.53	11.08	7.37	10.40	8.41	8.07	8.32
5s	8.59	11.25	7.48	10.53	8.44	7.91	8.22
5p	8.69	11.35	7.56	10.61	8.55	7.97	8.29
5d	8.80	11.55	7.87	10.87	8.84	8.47	8.27
6s	8.84	11.52	7.78	10.84	8.55	8.63	8.86
6p	8.90	11.57	7.82	10.88	8.57	8.04	8.41
MAE		2.37	1.15	1.85	0.24	0.54	0.35
MSE		2.37	-1.15	1.85	0.07	-0.29	-0.06

Table S10: Triplet excitation energy (in eV) of atom Be. Experimental data were obtained from Ref S41

AO	Exp	LDA	BLYP	B3LYP	LOSC-LDA	LOSC-BLYP	LOSC-B3LYP
2p	2.72	1.59	1.38	5.04	1.86	1.54	1.88
3s	6.46	8.37	7.87	7.74	6.90	6.22	6.45
3p	7.30	9.24	8.73	8.63	7.70	7.01	7.26
3d	7.69	9.62	9.21	9.10	8.18	7.55	7.77
4s	8.00	10.52	10.05	9.83	8.08	7.49	7.80
4p	8.28	10.77	10.32	10.07	8.29	7.69	7.97
4d	8.42	10.92	10.48	10.23	8.43	7.86	8.12
5s	8.56	11.19	10.73	10.47	8.39	7.81	8.21
5p	8.69	11.29	10.85	10.59	8.48	7.94	8.31
5d	8.75	11.42	10.97	10.74	8.71	8.14	8.55
6s	8.82	11.49	11.06	10.78	8.53	8.02	8.41
6p	8.89	11.54	11.15	10.86	8.54	8.07	8.45
MAE		2.30	1.91	1.79	0.28	0.60	0.30
MSE		2.11	1.68	1.79	-0.04	-0.60	-0.29

Table S11: Singlet excitation energy (in eV) of atom Mg. Experimental data were obtained from Ref S41

AO	Exp	LDA	BLYP	B3LYP	LOSC-LDA	LOSC-BLYP	LOSC-B3LYP
3p	4.35	5.00	5.61	5.13	4.62	5.28	4.86
4s	5.39	7.48	6.80	6.52	6.26	5.44	5.51
3d	5.75	8.33	8.21	7.63	7.02	6.79	6.48
4p	6.12	8.37	7.75	7.48	6.94	6.22	6.26
5s	6.52	9.00	8.52	8.19	6.96	6.41	6.57
4d	6.59	9.26	8.96	8.55	7.29	6.74	6.94
5p	6.78	9.29	8.83	8.50	7.25	6.70	6.89
6s	6.97	9.55	9.21	8.84	7.27	6.90	7.03
5d	6.98	9.70	9.48	9.06	7.36	7.25	7.13
6p	7.09	9.72	9.39	9.02	7.75	7.07	7.38
7s	7.19	9.81	9.53	9.13	7.40	7.05	7.21
7p	7.26	9.88	9.59	9.20	7.44	7.06	7.27
MAE		2.37	2.07	1.69	0.55	0.26	0.21
MSE		2.37	2.07	1.69	0.55	0.16	0.21

Table S12: Triplet excitation energy (in eV) of atom Mg. Experimental data were obtained from Ref S41

AO	Exp	LDA	BLYP	B3LYP	LOSC-LDA	LOSC-BLYP	LOSC-B3LYP
3p	2.71	2.64	2.57	2.61	2.36	2.19	2.36
4s	5.11	7.03	6.67	6.45	5.69	5.21	5.39
3d	5.95	7.22	7.03	6.93	6.07	5.63	5.88
4p	5.93	8.05	7.62	7.37	6.66	6.09	6.22
5s	6.43	8.90	8.47	8.15	6.96	6.37	6.53
4d	6.72	9.08	8.65	8.35	7.23	6.65	6.79
5p	6.73	9.20	8.78	8.46	7.16	6.65	6.82
6s	6.93	9.50	9.17	8.81	7.29	6.87	7.03
5d	7.06	9.62	9.26	8.92	7.47	7.04	7.21
6p	7.07	9.64	9.35	8.98	7.42	6.99	7.16
7s	7.17	9.79	9.50	9.11	7.41	7.04	7.21
7p	7.25	9.86	9.57	9.19	7.44	7.04	7.23
MAE		2.13	1.82	1.54	0.40	0.15	0.14
MSE		2.12	1.80	1.52	0.34	-0.11	0.06

Supplementary polyacene geometry

Benzene

12

C	0.0000	1.3966	0.0000
C	1.2095	0.6983	0.0000
C	1.2095	-0.6983	0.0000
C	0.0000	-1.3966	0.0000
C	-1.2095	-0.6983	0.0000
C	-1.2095	0.6983	0.0000
H	0.0000	2.4836	0.0000
H	2.1509	1.2418	0.0000
H	2.1509	-1.2418	0.0000
H	0.0000	-2.4836	0.0000
H	-2.1509	-1.2418	0.0000
H	-2.1509	1.2418	0.0000

Naphthalene

18

C	0.0	0.714951	0.0
C	0.0	-0.714951	0.0
C	2.426869	0.706561	0.0
C	-2.426869	0.706561	0.0
C	2.426869	-0.706561	0.0
C	-2.426869	-0.706561	0.0
C	1.242318	1.398661	0.0
C	-1.242318	1.398661	0.0
C	1.242318	-1.398661	0.0

C	-1.242318	-1.398661	0.0
H	3.369050	1.241625	0.0
H	-3.369050	1.241625	0.0
H	3.369050	-1.241625	0.0
H	-3.369050	-1.241625	0.0
H	1.241411	2.483152	0.0
H	-1.241411	2.483152	0.0
H	1.241411	-2.483152	0.0
H	-1.241411	-2.483152	0.0

Anthracene

24

C	0.0	1.220369	0.720788
C	0.0	-1.220369	0.720788
C	0.0	1.220369	-0.720788
C	0.0	-1.220369	-0.720788
C	0.0	0.0	1.400039
C	0.0	0.0	-1.400039
C	0.0	2.474059	1.403168
C	0.0	-2.474059	1.403168
C	0.0	2.474059	-1.403168
C	0.0	-2.474059	-1.403168
C	0.0	3.650786	0.711379
C	0.0	-3.650786	0.711379
C	0.0	3.650786	-0.711379
C	0.0	-3.650786	-0.711379
H	0.0	0.0	2.485281

H	0.0	0.0	-2.485281
H	0.0	2.473747	2.487567
H	0.0	-2.473747	2.487567
H	0.0	2.473747	-2.487567
H	0.0	-2.473747	-2.487567
H	0.0	4.594838	1.243045
H	0.0	-4.594838	1.243045
H	0.0	4.594838	-1.243045
H	0.0	-4.594838	-1.243045

Tetracene

30

C	0.0	0.724345	0.0
C	0.0	-0.724345	0.0
C	1.232442	1.402849	0.0
C	-1.232442	1.402849	0.0
C	1.232442	-1.402849	0.0
C	-1.232442	-1.402849	0.0
C	2.443772	0.724216	0.0
C	-2.443772	0.724216	0.0
C	2.443772	-0.724216	0.0
C	-2.443772	-0.724216	0.0
C	3.702747	1.405473	0.0
C	-3.702747	1.405473	0.0
C	3.702747	-1.405473	0.0
C	-3.702747	-1.405473	0.0
C	4.875977	0.713742	0.0

C	-4.875977	0.713742	0.0
C	4.875977	-0.713742	0.0
C	-4.875977	-0.713742	0.0
H	1.232720	2.487982	0.0
H	-1.232720	2.487982	0.0
H	1.232720	-2.487982	0.0
H	-1.232720	-2.487982	0.0
H	3.702863	2.489850	0.0
H	-3.702863	2.489850	0.0
H	3.702863	-2.489850	0.0
H	-3.702863	-2.489850	0.0
H	5.820918	1.243786	0.0
H	-5.820918	1.243786	0.0
H	5.820918	-1.243786	0.0
H	-5.820918	-1.243786	0.0

Pentacene

36

C	0.0	1.223172	0.726794
C	0.0	-1.223172	0.726794
C	0.0	1.223172	-0.726794
C	0.0	-1.223172	-0.726794
C	0.0	3.668639	0.726066
C	0.0	-3.668639	0.726066
C	0.0	3.668639	-0.726066
C	0.0	-3.668639	-0.726066
C	0.0	2.461665	1.404459

C	0.0	-2.461665	1.404459
C	0.0	2.461665	-1.404459
C	0.0	-2.461665	-1.404459
C	0.0	6.101733	0.714980
C	0.0	-6.101733	0.714980
C	0.0	6.101733	-0.714980
C	0.0	-6.101733	-0.714980
C	0.0	4.930253	1.406708
C	0.0	-4.930253	1.406708
C	0.0	4.930253	-1.406708
C	0.0	-4.930253	-1.406708
C	0.0	0.0	1.404933
C	0.0	0.0	-1.404933
H	0.0	2.462192	2.489563
H	0.0	-2.462192	2.489563
H	0.0	2.462192	-2.489563
H	0.0	-2.462192	-2.489563
H	0.0	7.047138	1.244171
H	0.0	-7.047138	1.244171
H	0.0	7.047138	-1.244171
H	0.0	-7.047138	-1.244171
H	0.0	4.930599	2.491074
H	0.0	-4.930599	2.491074
H	0.0	4.930599	-2.491074
H	0.0	-4.930599	-2.491074
H	0.0	0.0	2.489940
H	0.0	0.0	-2.489940

Hexacene

42

C	0.728760	0.0	0.0
C	-0.728760	0.0	0.0
C	1.406190	1.229341	0.0
C	-1.406190	1.229341	0.0
C	1.406190	-1.229341	0.0
C	-1.406190	-1.229341	0.0
C	0.728192	2.447851	0.0
C	-0.728192	2.447851	0.0
C	0.728192	-2.447851	0.0
C	-0.728192	-2.447851	0.0
C	1.405376	3.689513	0.0
C	-1.405376	3.689513	0.0
C	1.405376	-3.689513	0.0
C	-1.405376	-3.689513	0.0
C	0.727090	4.894222	0.0
C	-0.727090	4.894222	0.0
C	0.727090	-4.894222	0.0
C	-0.727090	-4.894222	0.0
C	1.407386	6.157229	0.0
C	-1.407386	6.157229	0.0
C	1.407386	-6.157229	0.0
C	-1.407386	-6.157229	0.0
C	0.715651	7.327785	0.0
C	-0.715651	7.327785	0.0
C	0.715651	-7.327785	0.0

C	-0.715651	-7.327785	0.0
H	2.491162	1.229591	0.0
H	-2.491162	1.229591	0.0
H	2.491162	-1.229591	0.0
H	-2.491162	-1.229591	0.0
H	2.490467	3.690188	0.0
H	-2.490467	3.690188	0.0
H	2.490467	-3.690188	0.0
H	-2.490467	-3.690188	0.0
H	2.491747	6.157716	0.0
H	-2.491747	6.157716	0.0
H	2.491747	-6.157716	0.0
H	-2.491747	-6.157716	0.0
H	1.244383	8.273439	0.0
H	-1.244383	8.273439	0.0
H	1.244383	-8.273439	0.0
H	-1.244383	-8.273439	0.

References

- (S1) Li, C.; Zheng, X.; Su, N. Q.; Yang, W. Localized orbital scaling correction for systematic elimination of delocalization error in density functional approximations. *National Science Review* **2017**, *5*, 203–215.
- (S2) Dunlap, B. I.; Connolly, J.; Sabin, J. On some approximations in applications of X α theory. *The Journal of Chemical Physics* **1979**, *71*, 3396–3402.
- (S3) Vahtras, O.; Almlöf, J.; Feyereisen, M. Integral approximations for LCAO-SCF calculations. *Chemical Physics Letters* **1993**, *213*, 514–518.

- (S4) Blase, X.; Attaccalite, C.; Olevano, V. First-principles GW calculations for fullerenes, porphyrins, phtalocyanine, and other molecules of interest for organic photovoltaic applications. *Physical Review B* **2011**, *83*, 115103.
- (S5) Potentials, A. I. Electron Affinities of Acceptor Molecules III: A Benchmark of GW Methods Knight. *Joseph W* 615–626.
- (S6) Schmidt, W. Photoelectron spectra of polynuclear aromatics. V. Correlations with ultraviolet absorption spectra in the catacondensed series. *The Journal of Chemical Physics* **1977**, *66*, 828–845.
- (S7) Clark, P. A.; Gleiter, R.; Heilbronner, E. Photoelectron spectra of planar sulfur heterocycles. *Tetrahedron* **1973**, *29*, 3085–3089.
- (S8) Eland, J. Photoelectron spectra of conjugated hydrocarbons and heteromolecules. *International Journal of Mass Spectrometry and Ion Physics* **1969**, *2*, 471–484.
- (S9) Liebsch, T.; Plotzke, O.; Hentges, R.; Hempelmann, A.; Hergenhahn, U.; Becker, U.; Viefhaus, J.; Heiser, F.; Xu, Y. Photoelectron spectroscopy of free fullerenes. *Journal of electron spectroscopy and related phenomena* **1996**, *419*–422.
- (S10) Ruscic, B.; Kovac, B.; Klasinc, L.; Güsten, H. Photoelectron Spectroscopy of Heterocycles, Fluorene Analogues. *Zeitschrift Naturforschung Teil A* **1978**, *33*, 1006–1012.
- (S11) Dupuis, P.; Roberge, R.; Sandorfy, C. The very low ionization potentials of porphyrins and the possible role of rydberg states in photosynthesis. *Chemical Physics Letters* **1980**, *75*, 434–437.
- (S12) Berkowitz, J. Photoelectron spectroscopy of phthalocyanine vapors. *The Journal of Chemical Physics* **1979**, *70*, 2819–2828.

- (S13) Gruhn, N. E.; Lichtenberger, D. L.; Ogura, H.; Walker, F. A. Reevaluation of the gas-phase valence photoelectron spectra of octaethylporphyrin and tetraphenylporphyrin. *Inorganic Chemistry* **1999**, *38*, 4023–4027.
- (S14) Boschi, R.; Murrell, J.; Schmidt, W. Photoelectron spectra of polycyclic aromatic hydrocarbons. *Faraday Discussions of the Chemical Society* **1972**, *54*, 116–126.
- (S15) Dori, N.; Menon, M.; Kilian, L.; Sokolowski, M.; Kronik, L.; Umbach, E. Valence electronic structure of gas-phase 3, 4, 9, 10-perylene tetracarboxylic acid dianhydride: Experiment and theory. *Physical Review B* **2006**, *73*, 195208.
- (S16) Palmer, M. H.; Findlay, R. H.; Ridyard, J. N. A.; Barrie, A.; Swift, P. The electronic structure of heteroaromatic molecules; non-empirical calculations and photoelectron spectra for the isomeric-thiazoles and-thiadiazoles. *Journal of Molecular Structure* **1977**, *39*, 189–205.
- (S17) Schäfer, W.; Schweig, A.; Gronowitz, S.; Taticchi, A.; Fringuelli, F. Reversal in the sequence of two highest occupied molecular orbitals in the series thiophen, selenophen, and tellurophen. *Journal of the Chemical Society, Chemical Communications* **1973**, 541–542.
- (S18) Brundle, C.; Robin, M.; Kuebler, N. Perfluoro effect in photoelectron spectroscopy. II. Aromatic molecules. *Journal of the American Chemical Society* **1972**, *94*, 1466–1475.
- (S19) Kimura, K. *Handbook of HeI photoelectron spectra of fundamental organic molecules*; Halsted Press, 1981.
- (S20) Rabalais, J. Photoelectron spectroscopic investigation of the electronic structure of nitromethane and nitrobenzene. *The Journal of Chemical Physics* **1972**, *57*, 960–967.
- (S21) Maier, J. P.; Muller, J.-F.; Kubota, T.; Yamakawa, M. Ionisation Energies and the

Electronic Structures of the N-oxides of Azanaphthalenes and azaanthracenes. *Helvetica Chimica Acta* **1975**, *58*, 1641–1648.

- (S22) Galasso, V.; Colonna, F.; Distefano, G. Photoelectron spectra of 1, 2-indandione, 1, 3-indandione and heterocyclic analogues. *Journal of Electron Spectroscopy and Related Phenomena* **1977**, *10*, 227–237.
- (S23) Ikemoto, I.; Samizo, K.; Fujikawa, T.; Ishii, K.; Ohta, T.; Kuroda, H. Photoelectron spectra of Tetracyanoethylene (TCNE) and Tetracyanoquinodimethane (TCNQ). *Chemistry Letters* **1974**, *3*, 785–790.
- (S24) Dougherty, D.; McGlynn, S. Photoelectron spectroscopy of carbonyls. 1, 4-Benzoquinones. *Journal of the American Chemical Society* **1977**, *99*, 3234–3239.
- (S25) Neijzen, B.; De Lange, C. Photoelectron spectroscopy of mono-and dicyanobenzenes and their perfluoro derivatives. *Journal of Electron Spectroscopy and Related Phenomena* **1978**, *14*, 187–199.
- (S26) Fujikawa, T.; Ohta, T.; Kuroda, H. X-Ray Photoelectron Spectroscopy of the Molecules Containing the C≡ N Group. *Bulletin of the Chemical Society of Japan* **1976**, *49*, 1486–1492.
- (S27) Sauther, J.; Wüsten, J.; Lach, S.; Ziegler, C. Gas phase and bulk ultraviolet photoemission spectroscopy of 3, 4, 9, 10-perylene-tetracarboxylic dianhydride, 1, 4, 5, 8-naphthalene-tetracarboxylic dianhydride, and 1, 8-naphthalene-dicarboxylic anhydride. *The Journal of chemical physics* **2009**, *131*, 034711.
- (S28) Dougherty, D.; Lewis, J.; Nauman, R.; McGlynn, S. Photoelectron spectroscopy of azulenes. *Journal of Electron Spectroscopy and Related Phenomena* **1980**, *19*, 21–33.
- (S29) Millefiori, S.; Gulino, A.; Casarin, M. UV photoelectron spectra, reduction potentials

and MO calculations of intramolecularly hydrogen-bonded naphtoquinones. *Journal de chimie physique* **1990**, *87*, 317–330.

- (S30) Hino, S.; Kikuchi, K.; Achiba, Y. Photoelectron spectra of higher fullerenes and their potassium complexes. *Synthetic Metals* **1995**, *70*, 1337–1340.
- (S31) Potts, A.; Price, W.; Streets, D.; Williams, T. Photoelectron spectra of benzene and some fluorobenzenes. *Faraday Discussions of the Chemical Society* **1972**, *54*, 168–181.
- (S32) Boschi, R.; Clar, E.; Schmidt, W. Photoelectron spectra of polynuclear aromatics. III. The effect of nonplanarity in sterically overcrowded aromatic hydrocarbons. *The Journal of Chemical Physics* **1974**, *60*, 4406–4418.
- (S33) Gaussian 09, Revision D.01, M. J. Frisch, G. W. Trucks, H. B. Schlegel, G. E. Scuseria, M. A. Robb, J. R. Cheeseman, G. Scalmani, V. Barone, G. A. Petersson, H. Nakatsuji, X. Li, M. Caricato, A. Marenich, J. Bloino, B. G. Janesko, R. Gomperts, B. Mennucci, H. P. Hratchian, J. V. Ortiz, A. F. Izmaylov, J. L. Sonnenberg, D. Williams-Young, F. Ding, F. Lipparini, F. Egidi, J. Goings, B. Peng, A. Petrone, T. Henderson, D. Ranasinghe, V. G. Zakrzewski, J. Gao, N. Rega, G. Zheng, W. Liang, M. Hada, M. Ehara, K. Toyota, R. Fukuda, J. Hasegawa, M. Ishida, T. Nakajima, Y. Honda, O. Kitao, H. Nakai, T. Vreven, K. Throssell, J. A. Montgomery, Jr., J. E. Peralta, F. Ogliaro, M. Bearpark, J. J. Heyd, E. Brothers, K. N. Kudin, V. N. Staroverov, T. Keith, R. Kobayashi, J. Normand, K. Raghavachari, A. Rendell, J. C. Burant, S. S. Iyengar, J. Tomasi, M. Cossi, J. M. Millam, M. Klene, C. Adamo, R. Cammi, J. W. Ochterski, R. L. Martin, K. Morokuma, O. Farkas, J. B. Foresman, and D. J. Fox, Gaussian, Inc., Wallingford CT, 2016.
- (S34) van Setten, M. J.; Caruso, F.; Sharifzadeh, S.; Ren, X.; Scheffler, M.; Liu, F.; Lischner, J.; Lin, L.; Deslippe, J. R.; Louie, S. G., et al. GW 100: Benchmarking G 0

W 0 for molecular systems. *Journal of chemical theory and computation* **2015**, *11*, 5665–5687.

- (S35) Zheng, G.; Irle, S.; Morokuma, K. Performance of the DFTB method in comparison to DFT and semiempirical methods for geometries and energies of C₂₀–C₈₆ fullerene isomers. *Chemical physics letters* **2005**, *412*, 210–216.
- (S36) Dabo, I.; Ferretti, A.; Marzari, N. *First Principles Approaches to Spectroscopic Properties of Complex Materials*; Springer, 2014; pp 193–233.
- (S37) Chong, D.; Gritsenko, O.; Baerends, E. Interpretation of the Kohn–Sham orbital energies as approximate vertical ionization potentials. *The Journal of Chemical Physics* **2002**, *116*, 1760–1772.
- (S38) Yang, Y.; Peng, D.; Lu, J.; Yang, W. Excitation energies from particle-particle random phase approximation: Davidson algorithm and benchmark studies. *The Journal of Chemical Physics* **2014**, *141*, 124104.
- (S39) TURBOMOLE V7.2 2017, a development of University of Karlsruhe and Forschungszentrum Karlsruhe GmbH, 1989–2007, TURBOMOLE GmbH, since 2007; available from
<http://www.turbomole.com>.
- (S40) Schreiber, M.; Silva-Junior, M. R.; Sauer, S. P.; Thiel, W. Benchmarks for electronically excited states: CASPT2, CC2, CCSD, and CC3. *The Journal of chemical physics* **2008**, *128*, 134110.
- (S41) Kramida, A.; Yu. Ralchenko, Reader, J.; and NIST ASD Team, NIST Atomic Spectra Database (ver. 5.3), [Online]. Available: <http://physics.nist.gov/asd> [2017, September 3]. National Institute of Standards and Technology, Gaithersburg, MD., 2015.